# HYDROGEN PRODUCTION FROM WATER USING SOLAR CELLS POWERED NAFION MEMBRANE ELECTROLYZERS

**A Thesis Submitted to**
**The Graduate School of Engineering and Sciences of**
**İzmir Institute of Technology**
**In Partial Fulfillment of the Requirements for the Degree of**

**MASTER OF SCIENCE**

**in Energy Engineering**
**(Energy and Power Systems)**

**by**
**Ziya Can Aksakal**

**July 2007**
**İZMİR**

We approve the thesis of **Ziya Can Aksakal**

**Date of Signature**

…… **19 July 2007**

**Assist. Prof. Dr. Erol Şeker**
Supervisor
Department of Chemical Engineering
İzmir Institute of Technology

…… **19 July 2007**

**Assoc. Prof. Dr. Gülden Gökçen**
Co- supervisor
Department of Mechanical Engineering
İzmir Institute of Technology

…… **19 July 2007**

**Assist. Prof. Dr. Fikret İnal**
Department of Chemical Engineering
İzmir Institute of Technology

…… **19 July 2007**

**Prof. Dr. Tamerkan Özgen**
Department of Chemistry
İzmir Institute of Technology

…… **19 July 2007**

**Assist. Prof. Dr. Yusuf Selamet**
Department of Physics
İzmir Institute of Technology

…… **19 July 2007**

**Assoc. Prof. Dr. Gülden Gökçen**
Head of Department
İzmir Institute of Technology

……

**Prof Dr. M. Barış ÖZERDEM**

Head of the Graduate School

# ACKNOWLEDGEMENTS

This study was carried out at the program of Energy Engineering and at the department of Chemical Engineering, Izmir Institute of Technology during the years 2004-2007. The study was funded through the Department of Prime Ministry State Planning Organization

I express my warmest gratitude to my supervisors Dr. Gülden Gökçen and Dr. Erol Şeker for introducing me to the promising world of hydrogen and its related applications. Their endless supports and contributions throughout the course of this thesis encourage me to pull of this work.

I would like to thank Dr. Fikret İnal, Dr. Sacide Alsoy Altınkaya, Dr. Zafer İlken for their valuable teachings during my undergraduate and graduate.

I wish to thank Güler Narin for her patience and guidance on testing my hydrogen samples and wish to thank Mahir Tosun for his hard data gathering work in Iztech Weather Station and for his sharing.

I am grateful to the whole stuff of Department of Mechanical and Department of Chemical Engineering for their help and technical assistance.

I express my thanks to all my friends and colleagues; Serdar Özer, Özge Malay, Güler Aslan, Dane Ruscuklu, Erkin Gezgin for their friendship and for taking my mind out of the work from time to time.

Finally my special thanks go to my family Kerem Aksakal, Gülser Aksakal, Burhan Aksakal, Ziya Yavuz and Pervin Yavuz for their support.

# ABSTRACT


## HYDROGEN PRODUCTION FROM WATER USING SOLAR CELLS POWERED NAFION MEMBRANE ELECTROLYZERS

The aims of this thesis are two folds; to construct single and multi cell proton exchange membrane electrolyzers and to evaluate the performance of these electrolyzers powered by solar panels on Iztech campus. All other parts, except the purchased membrane electrode assemblies, were designed, manufactured and assembled in our labs.

In the construction of single and multiple cell proton exchange membrane electrolyzers, Nafion-117 based membrane electrode assemblies were used. Graphite bipolar plates, end plates, current collectors and gaskets were machined on institute's computer numerical controlled lathe.

In the first stage, a single cell electrolyzer with 20$cm^2$ available electrolysis surface areas was examined with a direct current power supply by varying current density (0-500mAmp/$cm^2$), water flow rate (0.05 to 0.5g/$cm^2$min), and temperature (30-50$^oC$). It was found that average cell voltage decreases from 2.18V at 30$^oC$ to 1.97V at 50$^oC$ when the current density is 500mAmp/$cm^2$. Since cell gaskets were softened and stick to the membrane above 50$^oC$ of operating temperature, temperatures higher than 50 $^oC$ could not be tested.

5 cell electrolyzer stack was constructed according to the final single cell design. It was observed that the stack could generate 388ml/min hydrogen under 500mAmp/$cm^2$ and 10.09V of the operating condition at 41.5$^oC$. When the stack was directly coupled with a solar array, voltage of the stack was found to vary from 7.5V to 12.5V and the current density changes from 0 to 1000mAmp/$cm^2$ with respect to the solar radiance of the day. This results in a voltage efficiency ranging from 98.7% to 60% based on the higher heating value of hydrogen. Electrolyzer powered by solar cells can generate up to 750ml/min hydrogen and total daily production could be as high as 350L per day but weather condition greatly affects the production rate. Together with the losses inside the electrolyzer, another important energy loss is due to voltage mismatches between PV array and electrolyzer in low solar irradiance during sunrise and sunset.

# ÖZET

## GÜNEŞ PİLLERİ İLE ÇALIŞAN NAFION MEMBRAN ELEKTROLİZÖRLER İLE SUDAN HİDROJEN ÜRETİMİ


Bu çalışmanın amaçları iki ana başlıkta incelemek gerekirse öncelikle proton geçirgen membran tipinde tek ve çok hücreli elektrolizörler imal etmek daha sonra da bu elektrolizörleri İzmir Yüksek Teknoloji Enstitüsü`nde kurulan fotovoltaik paneller ile biraraya getirerek kampüsümüzde güneş enerjisinden hidrojen üretmektir. Katalist kaplı membranlar haricinde, grafit ara ve son yüzeyler, sıkıştırma levhaları, silikon contalar vb. malzemelerin tamamı enstitümüzdeki bilgisayar kontrollü tezgahlarda yapılıp biraraya getirilerek tek ve çok hücreli elektrolizörler imal edilmiştir.

Yapılan bütün elektrolizörlerde DuPont firmasının Nafion-117 serisi membranları kullanılmış olup ilk aşamada 20 $cm^2$ aktif yüzey alanına sahip tek hücreli elektrolizörler imal edilmiştir. Değişen akım yoğunluğu (0-500mAmp/$cm^2$), çalışma sıcaklığı (30-50$^oC$) ve su beslemesinde 1-10gr/d hücre verimi gözlenmiştir. Görülmüştür ki 30$^oC$ de 2.18V olan ortalama hücre voltajı 50$^oC$ de 1.97V'a düşmüş daha da yüksek sıcaklılara çıkılmaya çalışıldığında hücre contaları eriyerek gaz kanallarını tıkamış ve membrana yapışmıştır.

İmal edilen son tek hücreli elektrolizör tasarımı baz alınarak 5 hücreli bir elektrolizör imal edilmiştir. 41.5$^oC$ de çalışır iken 500mAmp/$cm^2$ akım yoğunluğunda 10.09V gerilim ile çalıabilen bu elektrolizör aynı akım yoğunluğunda dakikada 388ml hidrojen çıkışı verebilmektedir. Aynı elektrolizöre fotovoltaik modüller ile enerji verilmiş ve mevsimsel deneyler sonucunda, elektrolizör akım yoğunluğunun 0 ile 1000mAmp/cm2 arası değişir iken gerilimin 7.5V ile 12.5V arasında değiştiği gözlemlenmiştir. Maksimum 750ml/d hidrojen üretebilen sistemin günlük üretimi hava koşullarına göre 50 ila 350L arasında değişmiştir.

Elektrolizörden kaynaklanan verim kayıplarının yanısıra, sistemdeki önemli bir başka enerji kaybı da elektrolizör çalışma voltaj aralığının fotovoltaik panellerin maksimum enerji üretim noktasındaki voltajına olan uzaklığından kaynaklanmıştır.

# TABLE OF CONTENTS

# LIST OF FIGURES

# LIST OF TABLES

# CHAPTER 1

# INTRODUCTION

World energy consumption was reported to be above 10.5 billion tones of oil equivalent in 2005 and also found that it was increasing due to both the world population growth and the increasing life standards of humans with an average of 2.5% every year since sixties (BP-WSR 2006). Almost ninety percent of the energy used in the world has been supplied from fossil fuels but it was estimated that the economically accessible fossil fuel resources would finish soon according to "Hubbert's Peak" theory. The theory tells that as the world's energy demand increases, the production rates of fossil fuels are increased. This relationship continues up to a time when there will be no economical fossil fuel reserves available and thus, after this time, the production of primary fuels starts to decrease and according to supply/demand relationship, the fuel prices start to increase (Hubbert 1956). Therefore, in recent years, studies on alternative fuels and renewable energy resources have been increased. Although there are many proposed energy conversion systems using alternative fuels, such as biomass, hydrogen or biodiesel, there is no unique and viable solution.

All the developing countries and many of the developed countries are using fossil fuels as their primary energy source (an average of 87.6% of energy supply comes from fossil fuels in 2005). 27.1%, 36.8% and 23.7% of worldwide energy needs are provided by coal, oil and natural gas respectively (BP-WSR 2006). In addition, nuclear and hydroelectric energies are also used but their contributions to world energy demand are not as significant as the fossil fuels since they can produce electricity and their contributions to energy supply are limited with electric consumption. In fact, the nuclear and hydroelectric energy usages provide 6.1% and 6.2% of the total energy demand, respectively. Power productions from renewable energy sources, such as solar, wind or wave with the exception of hydroelectric are insignificant as compared to that from fossil fuels power generation.

Although the energy demand is increasing continuously and fossil fuels are not renewable, United States Department of Energy claims that the world fossil fuel reserve to annual production ratio is not changing seriously due to the exploration of new fossil fuel

reserves (DOE-AEO 2006). According to British Petrol reports, the total proven oil could last for 40 years, the natural gas can last for 66 years and the coal reserves would be depleted in 164 years if the world continues to consume energy sources at the today's consumption rates (BP-WSR 2006). The thing overlooked is the easily accessible fossil reserves are almost depleted and the required utilization and capital costs per unit fossil fuel is increasing; hence it seems to be unfeasible to explore and use new fossil fuel areas in near future. Similarly, nuclear energy based on fission technology is not an alternative solution due to its low reserves and unresolved problems, such as handling and storage of highly toxic and carcinogenic wastes with very long half times. Also, hydroelectricity will not be able to meet the increasing energy usage because the electricity produced in dams can only supply 15% of the total electric demand if all the available potential water resources are used (DOE-AEO 2006).

Looking to the Hubbert's Peak phenomena from Turkey's perspective is not a heartwarming situation either. Similar to other developing countries Turkey's energy demand is increasing continuously. Though, fossil fuel reserves and the mining activities (except lignite) of the country are limited. The most important fossil reserve is coal which is roughly 9 billion tones where 8 billion is in the lignite form (WEB_3 2007). Hence, the economy in Turkey is very much dependent on oil and natural gas imports. Total oil equivalent primary energy consumption in Turkey is 91.5 million tons in 2006, where 30.0 million tones are from oil, 14.75 from natural gas 31.7 from coal and 8.8 from hydroelectricity (WEB_2 2007). The oil production in Turkey is 2.28 million tons in 2006 from oil reserves located near Hakkari and Batman which meets 7.6% of total oil consumption, also 0.98 billion cubic meter of natural gas production meets 3.6% of total natural gas consumption (WEB_2 2007). As a result, Turkey's energy production rate is much less than its consumption; thus Turkey is a fossil fuel (including coal) importer. Table 1.1 summarize the production and consumption of the energy sources in Turkey in 2004 according to Department of Energy and Natural Sources Ministry of Turkey (WEB_2 2007).

Table 1.1. Turkey`s energy usage as a function of the energy sources (WEB_2 2007).

| | Oil Mton | Natural Gas ($10^9$ $m^3$) | Coal (Mton) | | Hydro electric (TWh) | SUM of Mton oil equivalence |
|---|---|---|---|---|---|---|
| | | | Lignite | Hard coal | | |
| Consumption | 30.0 | 19.9 | 56.5 | 19.4 | 39.6 | 91.5 |
| Production | 2.28 | 0.7 | 55.3 | 2.2 | 39.6 | 25.2 |

In addition to the limited supply and related cost problems of the fossil fuels, the atmospheric $CO_2$ concentration has been increasing due to increasing fossil fuel consumption. It has been agreed by the scientific community that there is a correlation between the average atmospheric temperature of the world and the atmospheric concentration of $CO_2$ and has been found that the average atmospheric temperature is increasing with $CO_2$ concentration (Shi 2003). In fact, not only $CO_2$ but also the other gases with long atmospheric duration, such as methane, nitrous oxide and some fluorocarbons, cause greenhouse effect. The greenhouse effect is that the shorter-wavelength solar radiation emitted from the sun passes through atmosphere and causes earth to warm while a part of the absorbed radiation is reradiated back to the space through the atmosphere as long wave radiation but this long wavelength radiation is absorbed by greenhouses gases such as $CO_2$ in the atmosphere and reemitted to Earth; hence causing the lower atmosphere warmer. To stop the global warming, an international protocol called “Kyoto protocol” was accepted by many countries in 1997 to decrease the concentrations of the greenhouse gases in the atmosphere. Up until now, 169 countries (except United States and Australia) which are emitting 61.6% of greenhouse gases have accepted the Kyoto protocol. The countries who signed Kyoto protocol must decrease their $CO_2$ emission within the time period decided by the committee. In other words, the governments of these countries are supposed to produce power by emitting less greenhouse gases than the level that they emit now using either improved energy conversion technologies or alternative fuels with the current conversion technologies. Efforts have been towards using renewable energy sources, such as solar, wind, biomass and geothermal energies. Examples for the renewable resource

utilization are the million solar Roof project in California and the offshore windmill farms in Holland.

The proposed energy conversion systems to use renewable energy resources/sources are unfortunately unviable as compared to the well-known and cost effective energy conversion systems for the fossil fuels. Another problem with the renewable energy systems is their power production regimes are controlled by environmental conditions. For example windmills can only convert wind energy into electricity when it is windy. Similarly, photovoltaic panels can only convert solar energy into electricity during day times.

The energy conversion technologies based on the renewable energy sources/resources are most suitable for stationary applications, such as powering and heating of home or businesses. For vehicles, the direct applications of these conversion technologies are not straight forward and also not practical but novel materials for Li-Ion batteries or super capacitors that could be charged using electricity obtained from solar panels or windmills have been investigated to replace the gasoline engines with the electrical motors.

Among renewable energy sources, hydrogen as a synthetic fuel seems to be a viable solution for stationary and mobile applications. For example, hydrogen could be used in internal combustion engines with some modifications and also it could be used with various fuel cell systems to power vehicles or houses. Although it is the most abundant element in the universe, there is no natural pure hydrogen resource on earth and it is always bound to other substances. Therefore, hydrogen must be produced using other energy sources/resources. In fact, hydrogen is a secondary energy source which can be produced from primary energy sources. In other words, hydrogen is not the energy source but it is an energy carrier like electricity. It can be transferred from its production site to its usage areas via pipelines or could be used to be converted into other energy types, such as electricity or direct mechanical work. Hydrogen can be produced from all kind of fossil fuel types; for example through coal gasification or methane reforming or the pyrolysis of oils. It can be also produced via water electrolysis or other economically non-mature alternatives like photoelectrical and photobiological methods. Hydrogen production via thermochemical treatments of fossil fuels results with a significant amount of carbon dioxide release to the

atmosphere according to their hydrogen/carbon ratios. Today, hydrogen is commercially produced by the steam reforming of natural gas. Although methane among many fossils fuels has the lowest carbon content (hence leading to low emission of $CO_2$), natural gas reserves are inadequate to be accepted as a main fuel for future. In addition, hydrogen could be produced through coal gasification but the usage of coal causes the land, air and water pollutions. Similarly, nuclear energy could also be used to produce hydrogen but there are unresolved safety and radioactive waste disposal issues. Therefore, petroleum, coal, natural gas and nuclear resources are all potential sources of hydrogen but they are not clean and long-term solutions.

Energy conversion technologies, such as photovoltaic solar cells (from solar energy to electricity), wind turbines (from wind energy to electricity), small scale sustainable hydropower (from water potential to electricity), geothermal (from hot underground water to heat or electricity), are increasingly being used as alternative or supportive ways to replace traditional energy conversion technologies. These alternative renewable energy sources and their conversion technologies could be used to produce hydrogen via electrolysis to power up motor vehicles. This is important, since the internal combustion engines are responsible for one half of the air pollution. In the electrolysis process, water is split into hydrogen and oxygen by applying the necessary amount of current for the desired hydrogen production rate. There are two commercially available electrolyzer types. First one based on alkaline water electrolysis technology which is relatively well known and mature. The second one is the proton exchange membrane (PEM) electrolyzer. There are also other types of electrolyzers such as inorganic membrane electrolyzer or solid oxide electrolyzers as shown in Table 1.2 but their operation life time is very limited; thus they are premature to be compared with alkaline and PEM electrolyzers.

Table 1.2. Types of Electrolyzers

| | Cathode Material | Anode Material | Separation Media | Electrolyte | Working Temp |
|---|---|---|---|---|---|
| Conventional Alkaline Electrolyzer | Steel or Nickel | Nickel | Asbestos | 25-35% KOH | 50-60 |
| Advanced Alkaline Electrolyzer | Activated Nickel | Activated Nickel | Polymer reinforced asbestos | 25-35% KOH | 80-100 |
| Proton Exchange Membrane Electrolyzer | Pt, Ir, Ru coatings | Pt coating | Proton Exchange Membrane | Separation media acts as an solid electrolyte | 70-90 |
| Inorganic Membrane Electrolyzer | Nickel Sulfur | Cobalt | Polyantemon | 14-15% | 120-130 |
| Solid Oxide Electrolyzer | Nickel in Zirconium | Platinum Spots | - | solid ceramic electrolyte | 800-1000 |

Among the electrolyzers listed in Table 2, the proton exchange membrane (PEM) seems to be the most suitable electrolyzer to produce hydrogen using renewable energy sources because PEM electrolyzers can operate over a wide range of current density, hence making them suitable for integration with photovoltaic panels or wind turbines. PEM based electrolyzers are similar devices with PEM fuel cells being operated in reverse but the catalyst types and loadings on membrane surfaces are different. Moreover, unitized regenerative fuel cells can be used both in fuel cell and electrolyzer mode. PEM electrolyzers consist of membrane electrode assembly (MEA) (composed of PEM solid electrolyte with each side coated with suitable catalysts for the anode and the cathode), gas diffusion layers and electric current collectors. The electrolyte of PEM is a solid perfluorinated membrane being a barrier to keep hydrogen and oxygen gases separate during the electrolysis. In a PEM electrolyzer, water splits into oxygen and hydrogen through the overall reaction shown below in equation 1.1;

$$H_2O \longleftrightarrow H_2 + \frac{1}{2}O_2 \qquad (1.1)$$

The reaction goes through two half reactions called anode and cathode reactions under an applied potential across the MEA. The water decomposition reaction shown below in equation 1.2 occurs on the anode side;

$$H_2O \longleftrightarrow 2H^+ + \frac{1}{2}O_2 + 2e^- \tag{1.2}$$

Where water splits into oxygen, protons and electrons over a suitable catalyst on the anode and the protons go through PEM electrolyte to the cathode side while the electrons go to an external power supply in order to complete the electrical circuit. At the cathode side, the protons coming from the anode through PEM electrolyte react with electrons supplied by the external power supply on a suitable catalyst to produce hydrogen gas molecule with the following reaction equation 1.3;

$$2H^+ + 2e^- \longleftrightarrow H_2 \tag{1.3}$$

It seems that the water electrolysis is very straight forward to accomplish and also suitable for the integration with the renewable energy conversion technologies. But in practice, there are many obstacles needed to be overcome so that the integrated electrolysis systems are viable choice for the production of hydrogen. This is especially obvious for the stack electrolyzer cells which contain many single cells to achieve the desired level of hydrogen production rate. For example, uniform water distribution, durable and active catalysts and also good contact between catalyst and membrane could affect the efficiency of the electrolyzer cell. In addition to the basic material problems, the engineering know-how to construct the PEM electrolyzers plays the critical role on the overall electrolyzer efficiency.

The ultimate goal in this thesis is to achieve hydrogen production via photovoltaic panels using our own designed and constructed electrolysis stack in campus area. Thesis can be divided into two main parts. In the first part a single PEM electrolysis cell was constructed and effects of current density, temperature and water flow rate on voltage responses were investigated to find the working characteristic of a single electrolysis cell.

In the second part a multiple cell stack was constructed and integrated with photovoltaic array to evaluate cell performance with the optimum working condition findings that was found in the first part.

The thesis contains six chapters. Following with this introduction, a literature review on the production of hydrogen and also the PEM electrolyzer (from material development to thermodynamic analyses studies to the investigation of integration of PEMs with solar cells) is presented in details in Chapter II. In Chapter III, the specifications of the materials and also the procedures used to construct PEM electrolyzer and the integration with the solar panels are explained. In addition, the test methods to analyze the performance of the PEM electrolyzer using the bench scale power supply and also the solar panels are presented in this chapter. In Chapter four, the characteristic performance evaluation plots, such as the voltage versus the current density or the power density versus the current density and mass balance across the cell, are presented for the bench scale power supply operated and also the solar panels integrated electrolyzers. The parameters affecting their performances are discussed by considering the hydrogen production rates, the cell efficiency, the construction materials and also the cell construction way. Finally, the conclusions obtained in this study are listed in Chapter five which follows by some recommendations in same chapter.

# CHAPTER 2

# LITERATURE SURVEY

## 2.1. Hydrogen Production Methods

Today, most of the hydrogen is produced with the processes of coal extraction, oil pyrolysis and the catalytic steam reforming. Unfortunately, these fossil fuel depended hydrogen production methods release significant amount of $CO_2$ (a major green house gas) to atmosphere. To eliminate/decrease $CO_2$ emission from such processes, carbon sequestration approach could be integrated to these methods but the overall system efficiency was found to decrease. Hence, today, most of the commercial hydrogen production is obtained from the catalytic steam reforming of natural gas without carbon sequestration process. However, alternative hydrogen production techniques, such as biological systems, photocatalytic systems, renewable energy based electrolysis systems and nuclear power plant assisted high temperature steam electrolysis systems are available and currently they are either in research & development stage or locally under large scale system test.

Biological hydrogen could be produced by various bacterial methods such as direct biophotolysis, indirect biophotolysis, photo-fermentation, dark fermentation and water-gas shift reaction of photoheterotrophic bacteria. Certain photosynthetic bacteria produce hydrogen from water in their metabolic activities using light energy as an example for direct biophotolysis applications. It is reported that a green alga, such as Scenedesmus, produce molecular hydrogen under light after being kept under anaerobic and dark conditions (Melis and Melnicki 2006).

The fastest hydrogen synthesis rates were reported with mesophilic dark fermentation bacteria (Chang et al. 2002) and CO-oxidation bacteria (Zhu et al. 2002) at 121mmol and 96mmol of $H_2$ per liter of bioreactor per hour, respectively.

Unfortunately, the technology must overcome the limitation of oxygen sensitivity of the hydrogen-evolving enzyme in order to increase both the efficiency and gas purity. The

total efficiencies of the fermentation systems are very low at about 5-10%. Levin and coworkers calculated that 758$m^3$ of photo-fermentation bacteria tank were required to supply a necessary amount of $H^2$ to a 5kW PEM fuel cell. The volume could be decreased to 1.25$m^3$ for CO-oxidation bacteria bioreactor, and 1 $m^3$ for dark fermentation mesophilic bacteria (Levin et al. 2004). It is projected for photo-fermentation bacteria that their low investment costs could overcome this low efficiency problem. The major challenges for dark fermentation and CO-oxidation bacteria are the mass transfer problems of their bio-reactors. The researchers were not able to scale up the experiments because they cannot achieve high reactant gas concentrations for the bacteria in the solution. High volume hydrogen bioreactors require new reactor designs and may require radically new technologies.

Another way to produce hydrogen is to use water electrolysis which is electricity depended hydrogen production method. In general, electrolysis is a process that the ionic compound is dissolved in a solvent so that its ions are available in the liquid. Current is applied between a pair of inert electrodes immersed in the liquid. Each electrode attracts ions which are of the opposite charge. In the water electrolysis case, cations are hydrogen ions and anions are the oxygen atoms. The energy required to separate these ions, and cause them to migrate to the respective electrodes, is provided by an electrical power supply. Therefore electrolysis is an electricity depended process and it could be viable if the electricity is cheap.

Hydrogen production using electrolysis cannot be classified as a renewable method because it depends on the source of the electricity. For example, wind, solar PV, wave and geothermal energies can all be a source to produce renewable hydrogen using electrolysis while fossil or nuclear fuel based electricity depended electrolysis cannot be classified as renewable hydrogen production. The Figure 2.1 below categorizes the hydrogen production methods according to their energy source.

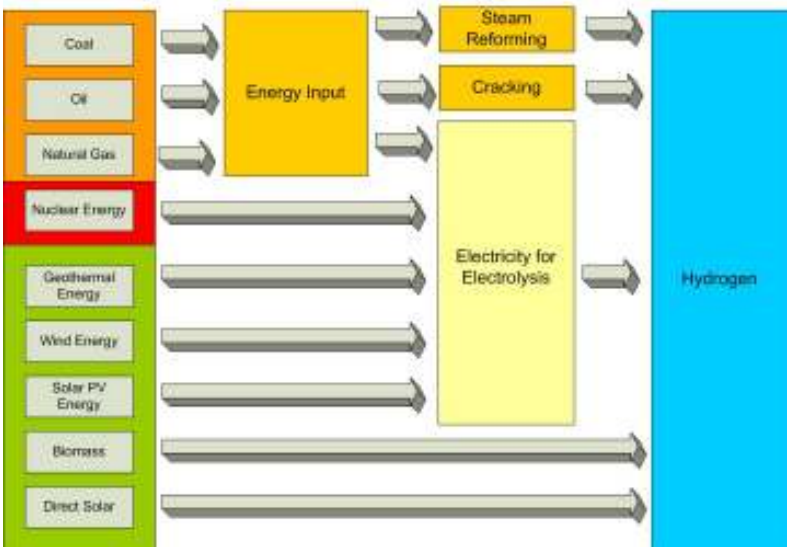


Figure 2.1. Various Sources for electrolysis

## 2.2. Electrolyzers

There are two mature electrolyzer types: Alkaline electrolyzers and Proton Exchange Membrane (PEM) electrolyzers.

Alkaline electrolyzers are the most commonly used electrolyzers in industry. Their hydrogen output is above 99% purity, although usually requires a further purification unit due to corrosive electrolyte vapor especially in fuel cell applications. Generally, 25 – 30 weight percent potassium hydroxide solution is used as a liquid electrolyte. Hydrogen production with this method has an efficiency of up to 80% (based on the high heating value of hydrogen). They are most effective when running on low current densities at about 0.3Amp/cm$^2$ or lower. However, disadvantages of this type of electrolyzers are their liquid electrolyte which is highly corrosive in high temperatures, thus resulting in relatively low electrolyzer lifetime (Barbir 2004).

The proton exchange membrane (PEM) fuel cell operated “in reverse” is actually a PEM electrolyzer. But the optimum operating conditions for the power and hydrogen production are significantly different than that one could expect to obtain from a PEM fuel cells operating in reverse. Although a lot of research and development was done on PEM

electrolyzers, the high cost of membrane, electrocatalyst (doped with noble metal, such as Pt, Ir, Ru), the requirement of highly "clean" water and a high cost of constructional materials limit the wide usage of this type electrolyzer. In spite of their high costs, there are several advantages of using PEM electrolyzers. They produce high purity (99.999%) hydrogen and oxygen (Grigoriev et al. 2006) which are very important for some applications, such as submarines and space shuttles. In addition, high purity hydrogen could be used in PEM fuel cells without requiring after-purification step unlike the alkaline electrolysis method. PEM electrolyzers could also work at high pressures up to 300 bar; thus reducing the compressor cost. Up until now, the most efficient electrolysis using PEM electrolyzers have been reported to operate at 1.556 cell voltage and 1Amp/$cm^2$ at $80^oC$ (Yamaguchi et al. 2000), hence achieving 95.1% efficiency (based on high heating value of hydrogen). Moreover, PEM electrolyzer can operate over a wide range of temperature, pressure and current density as compared to alkaline-type water electrolyzer (Tsutomu and Sakaki 2003). This unique feature makes PEM electrolyzers suitable for integrating with renewable energy sources which usually have variable electricity output due to their uncontrolled primary energy inputs. For example, the photovoltaic panels produce power proportional to solar intensity, which looks like a bell shape curve during the day or wind turbines produce power with the cubic function of the wind speed. Thus, hydrogen production based on PEM technology is a promising option for many renewable sources as it stores the uncontrolled production of electricity.

There are some difficulties with PEM electrolysis that need to be addressed before being a viable choice of power generation for future "hydrogen economy". The most obvious and commonly known obstacle is cheap electricity supply for electrolysis reaction. Theoretical electricity equivalent of 1kg hydrogen is about 40kWh, which is the main hydrogen production cost. In order to reduce the electricity cost of the electrolysis operation, researchers all over the world are trying to combine electrolyzers and renewable electricity generators with more efficient coupling methods (Bilgen 2000, Ahmad et al. 2006). Also electrolyzers are being interconnected to currently available grid system during the off-peak period to increase the load factor of the electric grid and use less expensive electricity (Oi and Sakaki 2003). Another way of reducing the electricity usage is to increase the efficiency of electrolyzers. Improvement of the membrane material and the

electrode design are being sought to reduce the inner resistances, hence increasing the cell efficiency. Mathematical models (Choi et al. 2004) and experimental works (Millet et al, 1989) points out that the electrical processes inside the cell show that the biggest voltage loss in an electrolysis cell occurs due to the anode overpotential while the cathode overpotential is relatively small due to fast reaction kinetics of hydrogen ions on platinum.

Decreasing the gas diffusivity and ohmic resistance of the membrane and increasing the ionic conductivity are currently under investigation by many research groups in the world. Besides, the relatively short operation life time of PEM electrolyzers (about 5000h), a high cost of membrane and noble metal coated electrodes and also high assembly cost (due to non-automated small scale production) are other obstacles needed to be solved for the renewable electricity powered PEM electrolyzers to be accepted as a mature technology.

### 2.2.1. Proton Exchange Membrane Electrolyzers

The working principle of PEM, reactions on each electrode and thermodynamics of the cell need to be known to better understand the PEM electrolyzers. Briefly, water electrolysis is a chemical reaction where water is the reactant whereas hydrogen and oxygen are the products. The electrolysis cell is a reaction medium composed of membrane electrode assembly (MEA), the electric current collectors, the gas distribution layers and the gaskets (Oi and Sakaki 2004). Unlike the alkaline electrolyzers, the electrolyte of a PEM electrolyzer is a solid perfluorinated membrane. Water is the only circulating liquid inside the cell although electrodes encountered an acidic environment equal to 20 wt% sulfuric acid solution owing to sulfonic acid groups of the membrane (Millet et al 1989). Mostly Nafion® (a trademark of DuPont) is used as proton exchange membrane. PEM is a solid electrolyte which is a barrier for both hydrogen and oxygen gases while it can transport protons and high current densities. Both sides of membrane are coated with noble metals which are usually Pt, Ir and Ru or some combinations of these metals. This catalyst coated membrane is called as membrane electrode assembly (MEA). Schematic representation of the parts of a single electrolysis cell is given in Figure 2.2.

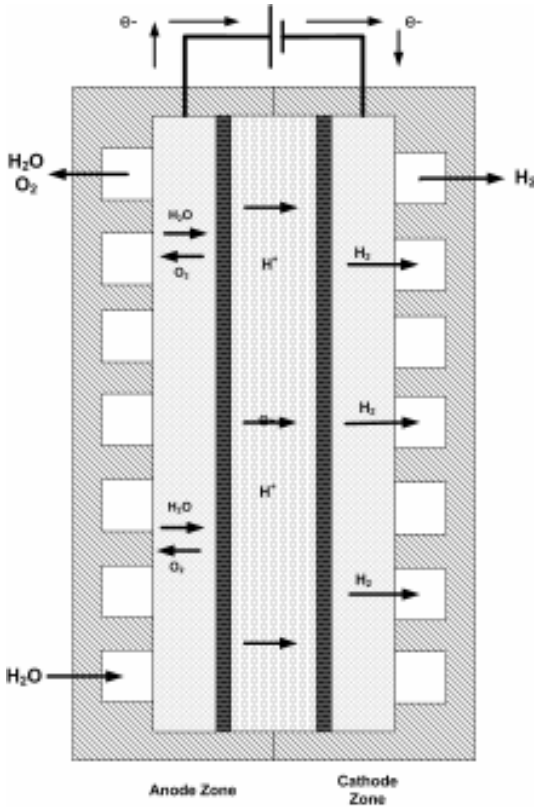


Figure 2.2. Schematic representation of a PEM electrolysis cell

De-ionized water must be used for PEM electrolysis in order to prevent the impurities and poisoning of the catalyst on each side. Water splits into oxygen, two protons and two electrons at the anode by applying a DC voltage higher than the thermoneutral voltage which is 1.481 V at standard temperature and pressure. Hydrogen ions (protons) pass through the proton exchange membrane and at the cathode they combine with electrons coming from the external power source to form hydrogen gas.

### 2.2.1.1. Thermodynamics of Proton Exchange Membrane Electrolysis

The formation of hydrogen and oxygen gases from liquid water is highly endothermic process; hence, resulting in a very low reaction rates, except at very high temperatures, such as 2000$^{o}$C. Total amount of energy which is the heat of reaction, $\Delta H$, is required to decompose water in the liquid phase and to expand the products in gas phase.

$$285{,}830\text{J/mol} + H_2O(l) \rightarrow H_2(g) + \frac{1}{2}O_2(g) \tag{2.1}$$

However by applying the electricity water can be split into hydrogen and oxygen ions at lower temperatures, the dissociation of water requires the amount of electrical energy corresponding to ΔG of the water splitting reaction. The electrical potential proportional to reaction Gibbs free energy is required between the electrodes to initiate water decomposition. This voltage is found from the definition of Gibbs free energy. In fact, theoretically it is the minimum electrolysis voltage (i.e. the ideal fuel cell voltage). The summation of the required electrical potential to compensate the Gibbs free energy and entropy at a temperature is called the thermoneutral ($V_{TN}$) voltage at the standard temperature and pressure, it equals to;

$$V_{t,p} = \frac{-\Delta G_{t,p}}{nF} + \frac{T\Delta\Delta}{nF} = \frac{-\Delta H_{t,p}}{nF} = \frac{-(-285830)}{2\times 96485} = 1{,}481V \tag{2.2}$$

$V_{TN}$ is the voltage at which a perfectly insulated electrolyzer would operate. Thus, $V_{TN}$ is equal to the sum of higher heating value voltage corresponding to the energy required for the saturation of hydrogen and oxygen with water vapor (Oi and Sakaki 2004). The cell efficiency is found through using the thermoneutral voltage. In this case, $V_{TN}$ is divided by the actual voltage applied to the cell to obtain the efficiency of an electrolyzer (Oi and Sakaki 2004).

$$\eta = \frac{V_{TN}}{V_{ACT}} = \frac{1.481}{V_{ACT}} \tag{2.3}$$

Another way to find the efficiency of an electrolyzer is that the energy equivalent of hydrogen output is divided by the given energy as shown in the equation 2.4 below (Ahmad et al. 2006).

$$\eta_{electrolyzer} = \frac{E \times Q}{Volt \times Current} \tag{2.4}$$

Where E is the calorific value of hydrogen (J/ml) and Q is the hydrogen flow rate (ml/s).

The efficiency of an electrolyzer is found to decrease as the current density and corresponding $H_2$ production rate of the cell increases. This means that the required electrical potential increases as the current density increases. This is due to the irreversibility occurring in the cell, which can be divided as the activation losses, ohmic losses, mass transport and concentration losses and increasing crossover of products through membrane in the high reaction rates and the operating pressures. (Onda et al. 2003).

Typical PEM electrolysis cell voltage is reported to be around 2V and the commercial electrolyzers have an efficiency ranging from 65% to 80% (Barbir 2004). Although an electrolyzer can be operated at higher efficiencies (up to 95%), this condition requires a lower cell voltage which also lowers the current passes through the electrolyte and the hydrogen production rate (Grigoriev et al. 2006). This dilemma could be overcome with the utilization of an electrolyzer stack with the high efficiency. Although 70% of the hydrogen production cost in PEM electrolyzers is due to the cost of electricity, increasing the efficiency was reported to compensate the relatively high capital expense of a PEM electrolyzer (Grigoriev et al. 2006). The analysis reported by Larminie and Dicks 2003 shows that an electrolyzer needed to be optimized by considering the efficiency which in turn affected the unit production cost and also the utilization of electrolyzer which ultimately affected the initial investment of the device.

Operating temperature of an electrolyzer is another important parameter on the system design. From electrolysis thermodynamic equations, it is expected that as the temperature increases the cell voltage should decrease. Yim and coworkers investigated the temperature effect on PEM electrolyzer with a 4.0 mg/cm$^2$ Pt loaded electrodes for both anode and cathode. It was found that voltage decreased from 1900mV to 1700mV as the temperature increased from 50$^o$C to 80$^o$C at 500mAmp/cm$^2$ current density (Yim et al. 2004). However, it is known that lifetime of solid polymer electrolytes decreases and product crossover through membrane increases with the increasing temperature. Thus,

another optimization should be done between the electricity price, purchased membrane cost and the produced hydrogen price to find the ideal temperature for a PEM electrolyzer.

There are several theoretical models to explain the current voltage and temperature characteristics of PEM electrolyzers. Choi and coworkers model assumes that the efficiency of a single or a stack of electrolyzer cells could be affected by either component(s) or operating parameter(s) of the electrolyzer (Choi et al. 2004). In fact their model separates the components of electrolyzer and reveals its electric circuit equivalent. The model provides a fairly good relation between the voltage and the current in Nernst potential through the exchange current densities of anode and cathode electrodes according to Butler-Volmer kinetics.

### 2.2.1.2. Proton Exchange Membrane of an Electrolyzer Cell

Proton exchange membrane (PEM) is a proton conducting polymeric membrane which acts as an electrolyte for both the fuel cell and the electrolysis applications. The first PEM used in a fuel cell is developed by General Electric in early sixties for use in a space mission for NASA. This premature copolymer showed insufficient oxidative stability under its operating conditions and it could work properly for only 500h during the mission. A major breakthrough in PEM technology came up with the announcement of perfluorosulfonic acid membranes called Nafion® by DuPont in 1967. (Larminie and Dicks 2003).

Typically perfluorosulfonic acid membranes are poor proton conductors unless water is present in the medium. Therefore the hydration of PEM is very important with respect to the performance of the cell. Although this is important for fuel cells, it is usually not the case for the electrolysis applications since the one side of the membrane is always introduced with water as a reactant.

Einsla 2005 reported that a typical proton exchange membrane had to match the following requirements in order to be able to be used in fuel cells and electrolyzers;

- Good film-formation
- High proton conductivity (especially at low relative humidity)
- Low electronic conductivity
- Water retention above 100$^{o}$C
- Thermal, oxidative and hydrolytic stability
- Effective reactant separator
- Capable of fabrication into MEA's
- Mechanical durability at high temperature (80 – 140$^{o}$C) for long times

Formerly, DuPont (Nafion®), Dow, and Asahi (Aciplex® and Flemion®) perfluorosulfonic acid polymers have been considered as an unique and nearly optimal materials to serve as separators in both electrolyzers and PEM fuel cells. However, they cannot meet the most important requirement: The cost of a PEM (e.g. 600- 700 \$/m$^2$). Recently, some of the most promising candidates for proton exchange membranes have been reported as polyamides, poly(ether ketone)s, poly(arylene ether sulfone)s and polybenzimidazoles (Rikukawa and Sanui 2000). The advantages of using these new candidate materials are their lower cost as compared to well-known perfluorinated membranes, such as Nafion, the inclusion of polar groups to improve water uptake over a range of temperatures, and also the possibility of recycling of these new candidates by the conventional methods (Rikukawa and Sanui 2000). Although there are no commercial supply of these new types of PEM's in the market, there is a great effort to commercialize them, such as by Dais-Analytic Co. and Odessa Co. Also, the pioneering fuel cell maker, Ballard Co., is working with the Victrex USA Co. and Greenville Co. to produce alternative new membrane based on sulphonated polyaryletherketone resin supplied (WEB_3 2006). Nafion® is currently almost an industry standard with its various types. It is fabricated from a copolymer of tetrafluoroethylene (Teflon®) and perfluorinated monomers contain sulfonic acid groups. The general formulation of the Nafion® is given in Figure 2.3 below.

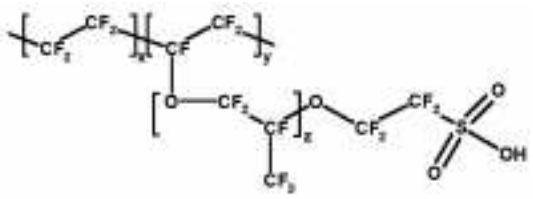

Figure 2.3. Molecular Formula of Nafion®

The hydrophilic regions around the clusters of sulphonated side chains enable water adsorption. The water adsorption process can increase the weight of membrane as much as 50%. Hydrogen ions are weakly attracted to the $SO_3^-$ group and they are able to move in these hydrated regions of the membrane. Though the hydrated regions are separate from each other, hydrogen ions able to move through the supporting structure but this situation decreases the proton conductivity. In a well hydrated membrane 20 water molecules could exist for each $SO_3^-$ side chain (Larminie and Dicks 2003). Thickness of the membrane is a crucial parameter because Einsla 2005 reported that as the thickness increased, the hydration of the membrane generally decreased which resulted in relatively poor ion conductivity. But as the thickness increased, the products, such as hydrogen, crossover decreased. Since the hydration of the membrane is usually not a problem in electrolysis application, thicker membranes are preferred for these devices.

### 2.2.1.3. Membrane Electrode Assembly and Electrode Structure of a Proton Exchange Membrane Electrolyzer Cell

The distance between the anode and the cathode reaction mediums increases the electrical resistance between these electrodes, thus reducing the cell efficiency drastically. Efforts to reduce the distance between these reaction mediums bring about the catalyst coated membranes which are known as membrane electrode assembly (MEA). Applying catalyst on both sides of the membrane minimize the distance between anode and cathode electrode, in fact the only media between anode and cathode reaction is the membrane

itself. The design minimizes the electrical resistances since the reaction occurs on both surface of the membrane due to the presence of the catalyst.

The definitions of anode and cathode electrodes are as follows; anode is “the electrode in a device that electrons flow out to return to the circuit” and the definition of cathode is “the electrode at which electrons go into a cell, tube or diode, whether driven externally or internally”. According to that, the cathode of the fuel cell is the side where water composes (oxygen side) and anode is the hydrogen inlet side. Though according to definition of cathode is the hydrogen generation side and anode is the side where water decomposes (Larminie and Dicks 2003).

Although PEM electrolyzer and PEM fuel cells seem similar devices they have significant differences such as, catalyst loadings and support material of their electrodes. Fabrication of membrane electrode assemblies for PEM electrolysis requires additional effort since duties of their electrodes are different than PEM fuel cell electrodes. The electrode in a fuel cell is used to expel the product water and to draw the reactant gases as quickly as possible whereas the idea behind an electrolyzer electrode is to draw the water and expel the gases as quickly as possible.

There are two alternative routes for the electrode fabrication used in PEM fuel cell and PEM electrolysis. First method is the separate electrode method which carbon supported catalyst is fixed with various techniques to a porous and conductive material, such as carbon cloth or carbon paper. Polytetrafluoroethylene (PTFE) is often be added for the fuel cell cathodes because it is hydrophobic and expels the product water (Larminie and Dicks 2003). The carbon paper cloth is also used to diffuse the gas through its pores onto the catalyst surface, which is called as the gas diffusion layer. Two similar electrodes are then fixed to each side of the proton exchange membrane (Larminie and Dicks 2003). The second method is to build electrodes directly onto the membrane. The catalyst is applied to the electrolyte with the methods, such as mechanical pressing, hot pressing, decal transfer, coating or clamping of precursors sol-impregnated electrode (Thangamuthu and Lin 2005). These fabrication approaches are used to achieve a good conduction of the catalyst surface with the proton exchange membrane which increases the effectiveness of the cell per unit mass of the catalyst. Although these methods are used for electrolysis MEA fabrication, catalyst and support materials may change in the electrolysis case, for example the

hydrophobic substances in electrodes will show worse performance due to the high resistance between the membrane and reactant water. Hydrophilic additives, such as Nafion®, are used to enhance the anode performances of electrolyzers (Ioroi et al. 2002).

At the beginning of PEM technology, the catalyst loading for both anode and cathode sides were as high as 28 mg/cm$^2$ of platinum (Larminie and Dicks 2003) where as 0.2mg/cm$^2$ or less is used now (Kim et al. 1998). Due to increased catalyst activity precious raw materials became only a small portion of both electrolyzer and fuel cells.

The kinetics of hydrogen on platinum is well known and shows that hydrogen evolution is the most efficient over platinum based catalyst material. Also, high current densities could be achieved at low overpotential with almost no mass transport limitation. Thus Pt is the most suitable catalyst for hydrogen generation on the cathode side of a PEM electrolysis cell. But there are some restrictions about platinum such as its sensitivity to poisoning gases like CO, COS and $H_2S$ above 10 ppm. (Levin et al. 2004). The models developed by Choi and coworkers shows that the overpotential of Pt coated cathode electrode is as small as 0.17 V at 1Amp/cm$^2$ for PEM electrolysis under standard conditions (Choi et al. 2004). Experimental works usually does not mention anode or cathode overpotential directly because of the experimental difficulties except Millet's found that the cathode overpotential changed from 0.15 V to 0.1 V with respect to Pt loading and temperature (Millet et al. 1992).

Different support and catalyst materials are used to investigate their effects on the total cell voltage (Grigoriev et al. 2006, Yim et al. 2003). There have been a lot of studies on electrodes and high efficient electrocatalysts for fuel cells and electrolyzers but they mainly focuses on anode electrode since the main energy losses occurs in water dissociation reaction.

Stable and active oxygen electrode is one of the key issue for the manufacture of electrolyzers. It is known that for oxygen reduction, platinum does not work well in the electrolyzer anode (Petersson et al. 2006). Thus, unlike fuel cell, the anode of the electrolyzer has different electrocatalyst, such as $IrO_2$, $RuO_2$, $SnO_2$ or their combinations (Grigoriev et al. 2006). These catalyst is usually mixed with $Ta_2O_5$, $TiO_2$ or $SnO_2$ to stabilize the structure (Rasten et al. 2003).

Ioroi et al. examined the effects of several additives, such as Nafion, PTFE, iridium, on the oxygen electrode of a regenerative fuel cell. They found out that as the PTFE content increased from 0 wt. % to 12 wt. %, the electrolysis cell voltage increased from 1900mV to 1950mV at 500mA/$cm^2$ current density. As it is expected hydrophobic effect of PTFE increases the cell voltage and also causes to decrease the voltage efficiency of the cell. However, Nafion as an additive to the anode electrode was found to have a favorable effect and in fact, 14 wt. % Nafion additive decreased the cell voltage up to 200mV at 500mA/$cm^2$ which equaled to an 8% increase in voltage efficiency. In addition, they reported that iridium content had the most significant effect for the electrolysis voltage. For example, even 1 wt% iridium additive was able to decrease the cell potential of 100mV and also 50 wt. % Ir loading decreased the cell potential up to 500mV at 500mA/$cm^2$. (Ioroi et al. 2002)

Grigoriev and coworkers showed that the activity of the electrode with 50% $RuO_2$ was better than that with pure $IrO_2$. They investigated four anode electrocatalysts which are summarized in Table 2.1.

Table 2.1. Electrode types versus Cell Potential

(Source: Grigoriev et al. 2006)

| Catalysts | Anode | Cathode | Potential at 1A/$cm^2$ |
|---|---|---|---|
| 1 | 2.4 mg/$cm^2$ Ir (100 wt %) | Pt30/C 2.0 mg/$cm^2$ | 1750 mV |
| 2 | 2.0 mg/$cm^2$ $RuO_2$-$IrO_2$-$SnO_2$ (30-32-38 wt %) | Pt30/C 2.0 mg/$cm^2$ | 1700mV |
| 3 | 2.4 mg/$cm^2$ Ir (100 wt %) | Pd40/C 2.4 mg/$cm^2$ | 1660mV |
| 4 | 2.0 mg/$cm^2$ $RuO_2$-$IrO_2$ (50:50 wt %) | Pt30/C 2.0 mg/$cm^2$ | 1650mV |

(Pt30/C: 30 wt% pf Pt on carbon carrier electrolysis temp:90$^oC$)

It is seen that $RuO_2$-$IrO_2$ loaded anode electrode shows the smallest cell potential with respect to others. Grigoriev and coworkers reported that electrolyzers were operated up to 10000 hour but they did not mention about the degradation of anode loadings (thus voltage increments) with respect to time which is another important parameter.

Different than Grigoriev's work, Yim and coworkers tried to make regenerative electrolyzers by adding Pt into anode electrode. Regenerative electrolyzer (or fuel cell) can generate oxygen and hydrogen when electricity available or can generate electricity when oxygen and hydrogen is available. In order to simplify the comparison between different anode catalyst loadings, 4.0mg/cm$^2$ Pt loaded cathode is used in all the experiments (Yim et al 2004). The catalyst types and their loadings are listed in Table 2.2.

Table 2.2. Electrodes versus Cell Potential

(Source: Yim et al. 2004)

| Catalysts | Anode | Cathode | Cell Potential at 500mA/cm$^2$ |
|---|---|---|---|
| 1 | 4.0mg/cm$^2$ Pt Black | 4.0mg/cm$^2$ Pt | 1820mV |
| 2 | 4.0mg/cm$^2$ Pt-Ir 50:50 wt.% | 4.0mg/cm$^2$ Pt | 1590mV |
| 3 | 4.0mg/cm$^2$ Pt-IrOx 50:50 wt.% | 4.0mg/cm$^2$ Pt | 1610mV |
| 4 | 4.0mg/cm$^2$Pt-Ru 50:50 wt.% | 4.0mg/cm$^2$ Pt | 1630mV |
| 5 | 4.0mg/cm$^2$Pt-RuOx 50:50 wt.% | 4.0mg/cm$^2$ Pt | 1820mV |
| 6 | 4.0mg/cm$^2$ Pt-Ru-Ir 50:45:5 wt.% | 4.0mg/cm$^2$ Pt | 1700mV |

(Electrolysis temperature: 60$^o$C )

Yim and coworkers showed that electrolysis cells which had Pt-Ir, Pt-IrOx and Pt-Ru in their anodes had smaller cell potential due to pure Pt, Pt-RuOx and Pt-Ru-Ir. Also the stability of Pt-Ir and Pt-IrOx coatings were far beyond than the others.

As it is seen from different findings in the literature, the anode side catalysts are still under development unlike Pt loadings on the cathode side.

The catalyst coated membranes named as membrane electrode assembly, views differ in such a way that the layered catalyst structure on the membrane is called as "electrode". From this point of view, the membrane electrode assemblies, MEA's are also proposed to be called as the catalyzed membrane assemblies, (CMA) (Hoogers 2002). There is a requirement for anode and cathode substrate between bipolar plates through the catalyst for a better gas diffusion and a current divider.

The gas diffusion layer must be a highly conductive material for both fuel cell and electrolysis applications. It must have a porous structure to bring the reactants to the PEM for fuel cell and to expel the products for the electrolysis. In the conventional fuel cells, the gas diffusion layers are usually porous carbon matrix, such as carbon cloth or carbon paper. However, this structure is not suitable for water electrolysis due to the oxidation of carbon with active oxygen species, such as oxygen atom or hydroxyl free radicals, at high positive potentials of anode (Song et al. 2006, Petersson et al. 2006).

Gas diffusion layer of an anode electrode should not be a hydrophobic material. Thus, PTFE loading generally decreases the efficiency of the cell similar to the PTFE loading effect on the catalyst layer (Ioroi et al. 2003). Woven metal cloths, expanded metal sheets, perforated metal sheets or metal foams which are made up of corrosive resistive metals, such as titanium, zirconium, hafnium, niobium and tantalum, are used as the electrolyzer gas diffusion plates (Petersson et al. 2006).

Another approach for making electrolysis gas diffusion layer is to promote the traditional carbon matrix used in the fuel cells with a suitable metal(s). This approach aims to form an oxygen molecule rapidly before the atoms starts to diffuse the gas diffusion layer (Song et al. 2006) proposed it as a new cathode for electrolysis cell which had a water reservoir placed inside the cell contacting with the membrane, and with the Toray carbon paper used as the gas diffusion layer. After the electrolysis operation, no corrosion of the oxygen electrode occurred because the water did not come in direct contact with the electrode and the active oxygen species were combined before reaching the gas diffusion layer. However, their cell structure was complicated and the gap between anode and cathode was wide which caused less voltage efficient electrolysis operation (Song et al 2006).

### 2.2.1.4. Bipolar Plates

All the fuel cells and electrolyzers (with the exception of laboratory bench scale ones) are constructed with many cells connected in series. Similar to the serially connected battery systems, the serially connected fuel cell systems could generate electricity at high

voltages. This concept is also valid for the electrolysis cells connected in series. The serially connected cells are called as “stack” and they could be operated at high voltages which are proportional to the number of cells. To connect cells in series, the anode side of one cell should connect with the cathode of another one. This can be achieved by wiring each cell with next one in the stack. In this way, current can pass from one cell to the next one but for a higher current rate (which is usually the case for electrolysis) the current distribution problems may occur. The other way to pass the current between cells is to construct an electric conductive plate which is called as bipolar plate. The name of the bipolar comes from this unwired stacking configuration where one side of the plate acts as the anode of the cell while the other side behaves as the cathode for the adjacent cell. Other duties of bipolar plates are that they have to supply water to the anode gas diffusion layer while dispelling the oxygen gas from electrode and also it has to dispel hydrogen gas from the cathode gas diffusion layer. These are major duties of a bipolar plate in an electrolyzer but also it has to be a good heat conductor to prevent the high temperatures inside the cell and it has to be made from a durable and high strength materials since the other parts of the cell are made up of low mechanical strength materials. A bipolar plate should have low permeability values for both oxygen and hydrogen to ensure that they are separate.

Metals can be used as bipolar plates since they are abundant and cheap although the most common material used for bipolar plates is graphite since it is a good thermal and electrical conductor like metals. Moreover, it is easy to machine the flow channels on graphite blocks with respect to other metals. Graphite is also less permeable to hydrogen than most of the metals.

Graphite bipolar plates constitute almost 88% of the electrolyzer and in particular coated metal bipolar plates constitute 81% by mass of a stack since the other parts are very thin (Li and Sabir 2004).

As department of energy (DOE) points out that, one of the main obstacles in front of the hydrogen economy is the low power density (according to internal combustion engines) of fuel cells and electrolyzers. Reducing the weight of bipolar plates can increase the power density significantly as it can be understood from its total weight sharing (DOE-HVR 2006).

Other than material specifications, the pattern of the channels on the plate is one of the most important issues for the fuel cells. Since there is no specific pattern published for electrolyzers, the subject has similar importance for the electrolyzers because the PEM electrolyzers are also devices where three phases, solid (electrocatalyst), liquid and gas, must be in a proper contact. Various possible flow field designs for the fuel cells were proposed during the development of fuel cells.

The simplest flow field design is the pin-type flow field which is a network formed by many fins arranged in a regular pattern. As a result of this design pin-type flow fields result in very low pressure drop (Reiser and Sawyer 1988). But, reactant flows through paths which have the least resistance. This situation leads to an inadequate reactant distribution which causes unbalanced current distribution and resulting in spatial temperature variations.

Studies to prevent the deficiencies of pin-type flow field have resulted in straight flow fields (Pollegri and Spaziante 1980). The design was further investigated by General Electric and Hamilton Standard. In this design separate parallel flow channels were connected to one inlet and one outlet of the field. The idea behind the design is to transmit the inlet pressure of the reactant in to the thin channels. Thus reactant can go all the way through the channel which prevents the inadequate reactant distribution. The pattern works well in the beginning but the deficiency of the pattern appears as the operating time increases. If water flow is obstructed or encountered with more resistance than other channels, the stagnant areas appear inside the cell. This situation results with similar problems as found in pin type flow field (Li and Sabir 2005).

Serpentine flow pattern were studied to overcome the heterogeneity developed in pin type and straight flow fields (Watkins et al. 1991). Watkins designed a pattern which have only one flow channel between inlet and outlet. In order to maximize the contact with MEA the channel were roamed from one side to other side several times. The design prevents the obstruction of flow since there is only one way to go for fluid although high reactant pressure losses occur due to very long flow channels. The pressure losses can be as much as 30% of the total stack power of fuel cells (Li and Sabir 2005). The concept was improved by various researchers to decrease the pressure drop such as multiple channel modified serpentine flows.

Interdigitated flow field is a different approach to flow field design. In other flow field designs, reactant and products are transported in bulk phase in the channels via pressure differences. Interdigitated flow field has a two parallel channel with dead ends. The reactant flows through the input channel network and also diffuses into the membrane to pass to the output channel network. The interdigitated flow field forces the reactants into the active layer of the electrode thus high power densities can be achieved (Wang and Liu 2004). Large pressure loss occurs for the reactant which limits the using area of this pattern with small stacks (Li and Sabir 2005).

Combining the observations from nature with interdigitated flow had led to some modification on this flow type. A similar pattern like the tissues of plant or in animal lungs was applied to the interdigitated flow field (Boff et al. 2006). Applying such a pattern of channels of different width and depth has a great advantage to distribute gases uniformly. The inventors have also realized that by forming sufficiently fine channels on the face of the flow field gas diffusion layers are becoming unnecessary for electrolyzers.

In addition to the flow patterns mentioned above, a gas diffusion layer without any flow channel or catalyst coated metal mesh (which is usually the case for PEM electrolyzers because of the reduced catalyst life due to the carbon deposition from carbon based layers) can be used for the distribution of reactants and collection of the products.

Various gas distribution methods have been shown to influence stack performances in fuel cells and electrolyzers like various catalyst loadings and different membranes. As the catalyst usage and membrane costs are reduced drastically, the cost of bipolar plates becomes a significant portion (up to 30%) of electrolyzer and fuel cell stacks (Li and Sabir 2004, Larminie and Dicks 2003).

### 2.2.1.5. Solar Powered PEM Electrolyzer Applications

PEM electrolyzer driven by the power of photovoltaic array is one of the promising hydrogen production methods just like wind turbines connected to the hydrogen generation systems. Photovoltaic (PV) cells turn the sunlight into electricity directly. Briefly, when the sunlight shines onto the semiconductor materials, the electrons in atoms of the

semiconductor leave and become free in the material so that they are carried externally through a load as a current (WEB_5 2006). These renewable systems generate electricity in fluctuated manners and this operating behavior makes them unsuitable for the power grid supply at high percentage sharing (Gonzales et al. 2003). However, for the electrolysis using renewable electricity, the load factor of these sources can be redounded. This combined usage concept to produce hydrogen has received considerable attention (Dıncer, 2002). Photovoltaic powered electrolysis applications are widely used all over the world although the efficiency of the photovoltaic panels could be as high as 15% (hence making them the most expensive electricity generators) (Torres et al. 1998, Ahmad and Sheneawy 2005).

Power generation from a photovoltaic panel is proportional to the sunlight intensity. In an open circuit, the panel can give the maximum voltage. But as the current taken from panels increases, the voltage of the panel starts to decrease. To overcome this problem, the modules are combined in such a way to obtain the maximum power. A successful PV powered electrolyzer system requires an electrolyzer design working at solar cells maximum power or vice versa. As discussed in the beginning of the chapter, voltage required for electrolysis increases as the current density increases. If the electrolysis curve could match as closely as possible with the maximum power point of the photovoltaic panels, a successful solar hydrogen generation seems to be doable. In the early work of Carpetis, the maximum power point line of a photovoltaic module and the solid polymer electrolyzer were plotted at varying voltages and currents. This study shows that a successful match between the electrolyzer and PV power line could increase the efficiency dramatically from 3.9% up to 5.5% (Carpetis 1984). Steeb and coworkers (1985) focused on maximum power point tracker called power conditioning. They pointed out that the power conditioning between PV's and the electrolyzers was not constant because the power generated by panels was not constant during the day and could fluctuate with weather conditions in a year. Also the power consumed by the electrolyzer is not constant due to the working temperature and degradation of components inside the cell. It is clear that even a successful match between an electrolyzer and photovoltaic source could be achieved; the maintaining this match in long term seemed not possible. A power conditioner decouples the source from the load and pushing to work them in different working points. The solar

generator is always working at its maximum power output point while the power given to the electrolyzer can be set according to its cell characteristics (Steeb et al. 1985).

In Aegean zone in Turkey, hydrogen generation by solar power driven electrolyzer was studied by Atagündüz et al. (Atagündüz, 1993). In this work the constructed electrolyzer is a 5 cell conventional alkaline one. Potassium hydroxide was used as the electrolyte and asbestos was used as the separation medium while nickel was used as electrode for anode and cathode. They tried to match the electrolysis unit with the PV panel maximum power point with a DC-DC converter. It was reported that the efficiency of the electrolyzer was about 80-87% while the converter efficiency was about 50%. The electrolyzer cell voltage changed between 3.5V to 4.5V.

# CHAPTER 3

# MATERIALS AND METHODS

Single and multiple cell electrolyzers were manufactured using the catalyst coated Ion-Power Co. membrane electrode assemblies (MEA). After that, manufactured stacks were powered by photovoltaic arrays to evaluate the solar hydrogen production ability on our campus.

MEA's were first tested in single cells and then tested in various stack formations in order to identify the possible problems easily and to eliminate the experimental difficulties such as the mixing of product gases, water leakage or obtaining uniform pressure through the MEA.

## 3.1. Materials and Equipments

Materials with their specifications used to prepare the electrolysis cell and stack are given in the table below.

Table 3.1. Properties of Materials used in Electrolysis Cell

| Materials | Specifications |
|---|---|
| Membrane Electrode Assembly (MEA) | Catalyst coated N-117 membrane (Ion Power) (70x70)mm total area |
| Gas Diffusion Layer (GDL) | 1 micron Pt coated 1.5 mm Titanium screen (45x45)mm |
| Bipolar Plate | Carbone Lorraine 1940PT Graphite Layer |
| Gaskets | temperature resistant 1mm thick silicon gaskets |
| Endplates | 8mm thick stainless steel plates (70x70)mm |
| Compression Bolts | 5mm diameter 8 steel bolts covered with plastic insulators |
| Electric Conduction Plates | 1mm thick TSE 554 copper plates |

DC regulated power source; GP1305TP of EZ Electronics was used to supply the required electrical energy for electrolysis cell and TES 2732 Universal data logger was used to

record the voltage and the current simultaneously for single and multi cell bench experiments. Power supply of the solar power driven electrolysis stack was an array which was consisted of six Siemens SM-55 photovoltaic panels connected in parallel. Current and voltage of these panels were measured by a DC power analyzer of CASE Electronics.

## 3.2. Methods

The experiments of this study can be categorized into two groups.

- To manufacture an electrolysis cell and investigate its optimum working conditions.
- To manufacture an electrolysis stack and couple it with photovoltaic panels to investigate the solar hydrogen production ability on Iztech campus.

### 3.2.1. Producing the PEM Electrolysis Cell

The design of a cell structure which supplies water and electricity while withdrawing oxygen and hydrogen simultaneously from membrane electrode assembly is critical. Carbon graphite plates were selected as construction materials due to their high electrical and heat conductivity and easy to machine properties. The plates were designed in Solid Works® and then transformed into a Parasolid model computer file to process in our institute's computer numerical controlled (CNC) lathe. 2D diagram of the proposed electrolysis cell design is given in Figure 3.1

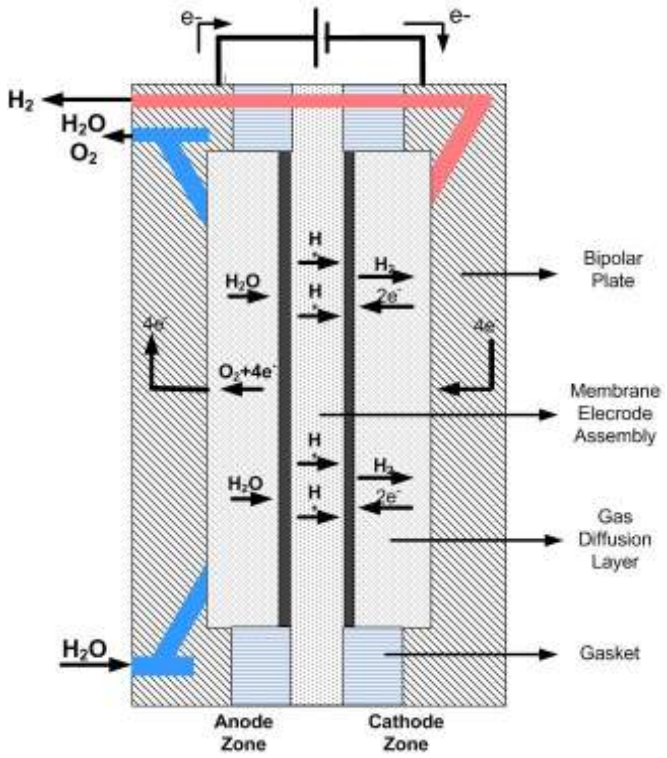


Figure 3.1. 2D Schematic Representation of an Electrolysis Cell

After various designs, an empty flow field is enough to support the metal screen and apply pressure uniformly; thus eliminating compression variations through the membrane. The porous screen structure of the gas diffusion layer transport the product gases and water from compartments to membrane electrode assembly (MEA) even in the absence of a specific flow pattern behind it. The proposed oxygen side can be seen in Figure 3.2.

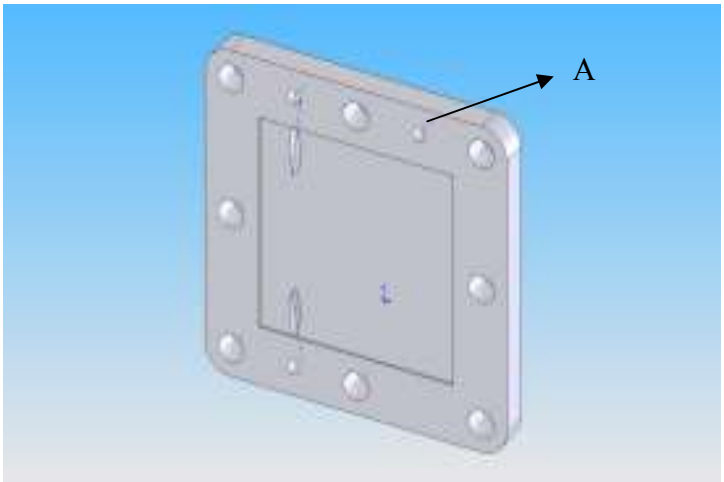


Figure 3.2. Anode side of the electrolysis cell

Water inlet and oxygen outlet holes were first drilled vertically and then connected diagonally to the empty part of the anode side to feed water and withdraw the generated oxygen with some unreacted water from the gas diffusion layer. Hydrogen output stream coming from cathode side and bypassed the anode zone through a hole, A.

Empty base design was used again for the cathode side to uniformly counterbalance the pressure on GDL. The hydrogen generation on the cathode catalyst surface cause a pressure increment which leads the gas to diagonally drilled hole on the graphite. Figure 3.3 shows the proposed cathode layer of the cell.

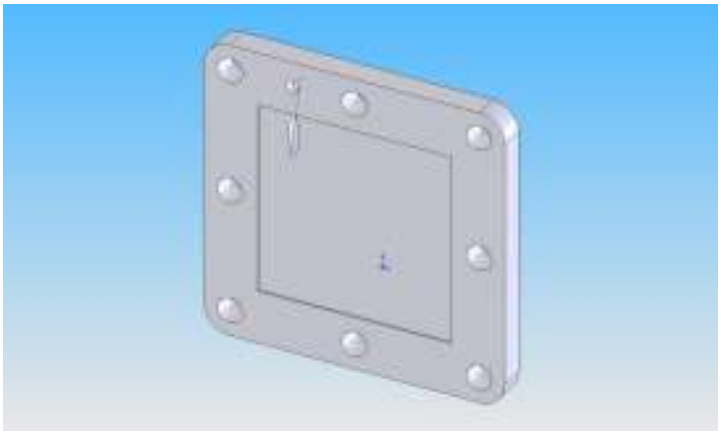

Figure 3.3. Cathode Side of the electrolysis cell

In order to level the surface of GDL with silicon gasket, depth of the fields was set to 0.5mm for both anode and cathode side. GDL's were placed into the field and gaskets were placed to the surroundings of GDL.

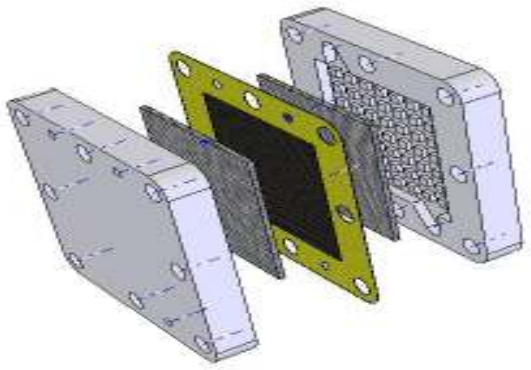

Figure 3.4. Parts of the Electrolysis Cell

Manufactured electrolysis cell was tightened with eight metric 5mm bolts. Metal bolts were sealed with plastic tubes to avoid the electrical conduction. 8mm thick stainless steel plates were also used at both ends to apply much uniform pressure on the components of the cell.

## 3.2.2. Assembly and Test Procedures for the PEM Electrolysis Cell

- **Single Cell PEM Electrolyzer Assembly Procedure**

1. Insert 6 bolts to the cathode side end plate and fix the plate to the bench.
2. Place a 1mm thick silicon layer on the end plate.
3. Place the copper electric conduction plate on silicon layer.
4. Place the cathode side graphite.
5. Place the cathode side GDL into the cathode graphite layer.

6. Cover the cathode GDL with 1mm thick silicon gasket.
7. Submerge the MEA into water and wait until the expansion of membrane stops.
8. Insert the wet MEA on GDL.
9. Place the anode side GDL on the anode graphite layer.
10. Cover the anode GDL with 1mm thick silicon gasket.
11. Place the anode side graphite with its mounted components on MEA.
12. Place the water inlet, hydrogen and oxygen outlet tubes into the anode graphite.
13. Place the copper plate on anode graphite.
14. Place a silicon layer on copper plate.
15. Fixate the anode side end plate.
16. Insert the cap screws to the bolts and tighten them diagonally.
17. Stick the thermocouple probe on to graphite.

After the assembly, deionized water was fed to the water inlet using peristaltic pump. To make sure that water filled up the inside of cell, filling should continue until flooding of water from oxygen output is observed. It takes 0.6 to 6 minutes according to the water feed rate since the inner volume of the cell is 6 $cm^3$. The oxygen output was connected to the inlet water reservoir in order to return the unreacted water to the system. Hydrogen output was connected to a gas liquid separator to separate the liquid water coming with hydrogen. Finally water vapor was adsorbed using silica gel filled bubbler from the hydrogen stream. Positive terminal was connected to the anode side, negative terminal was connected to the cathode side to apply the electricity from the power supply.

Current applied to the cell was increased gradually up to 10.13 Amp which is equal to 500mAmp/$cm^2$ for the proposed cell design. The other control variable, water flow rate, was changed from 1ml/min to 10 ml/min. Temperature and voltage was measured continuously. The setup of the single cell electrolysis experiment is given in Figure 3.5.

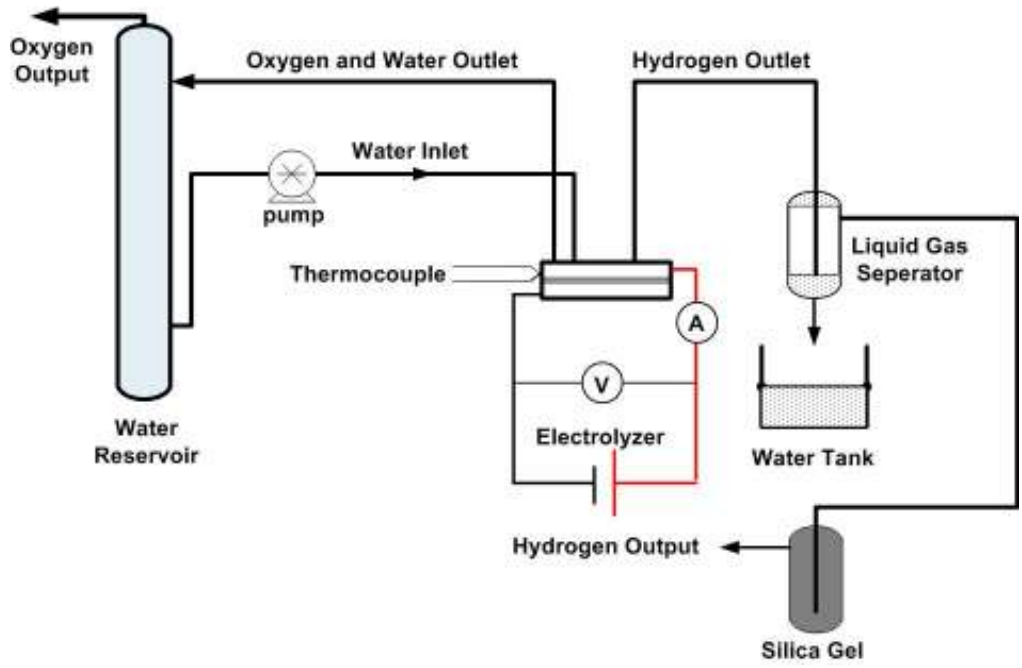


Figure 3.5. Single Cell Electrolysis Setup

Effects of the temperature and the flow rate on voltage-current density characteristics of the electrolysis cells were studied. Current given to the electrolyzer was increased with respect to time in each set. Potential difference between the electrodes, hydrogen and oxygen flow rates and water permeation through membrane, were recorded using voltmeter and digital soap bubble flow meters.

### 3.2.3 PEM Electrolysis Stack

The design is analogous to the single cell electrolyzer. In fact, first and last graphite plates, end plates, silicon gaskets, gas diffusion layers of the stack were identical with the plates used in single cell electrolyzer, though connecting two cells in serial requires an electrical conduction between the cathode and adjacent cells anode. Thus, the only difference from single cell electrolyzer is that two sided plates are used to achieve the conduction between cells. Both sides of these plates were machined to place anode and cathode GDL and appropriate ducts were drilled on plates to collect the product gases and

to deliver water. The front side of each plate is the cathode of the cell and the back side is the anode side of the adjacent cell. This two sided plates are named bipolar plates. Similar cell concept was applied to stack formation and the schematic representation of this formation is given in Figure 3.6.

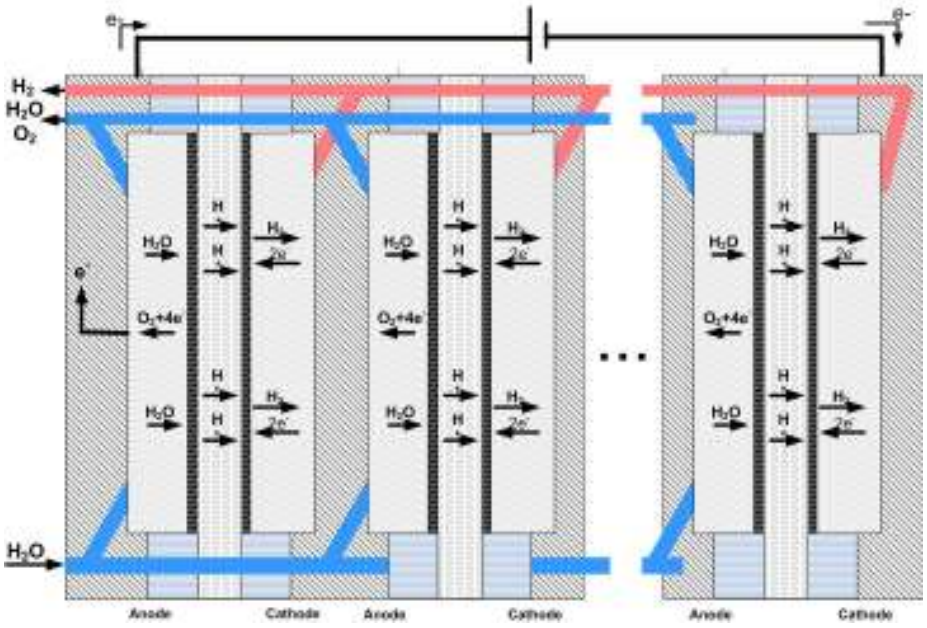


Figure 3.6. 2D Schematic of a PEM electrolysis stack

Front (cathode) and back (anode) side graphs of the proposed bipolar plate are given in the figure below.

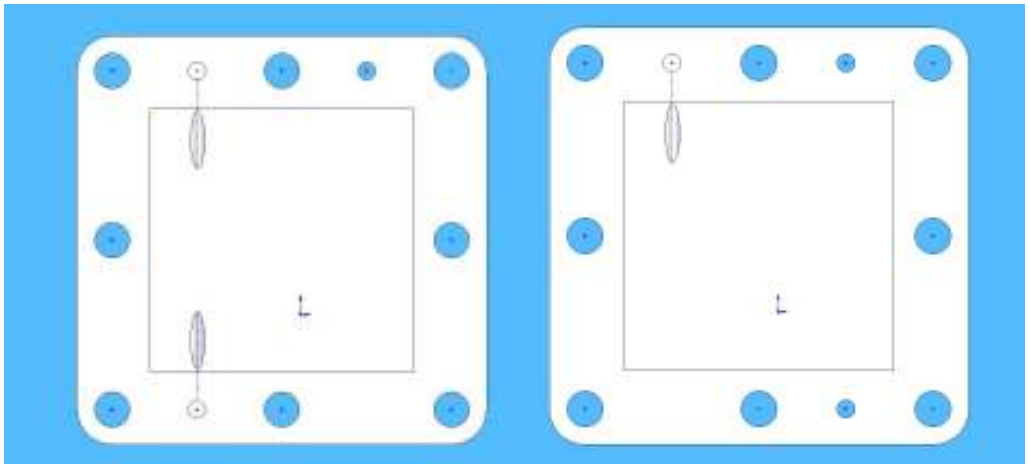

A B

Figure 3.7.a) Front Side of the Bipolar Plate b) Rear Side of the Bipolar Plate

An exploded, isometric Solid Works® drawing of the manufactured two cell electrolyzer stack is shown in the figure 3.8. The design was also applied for cell numbers up to six.

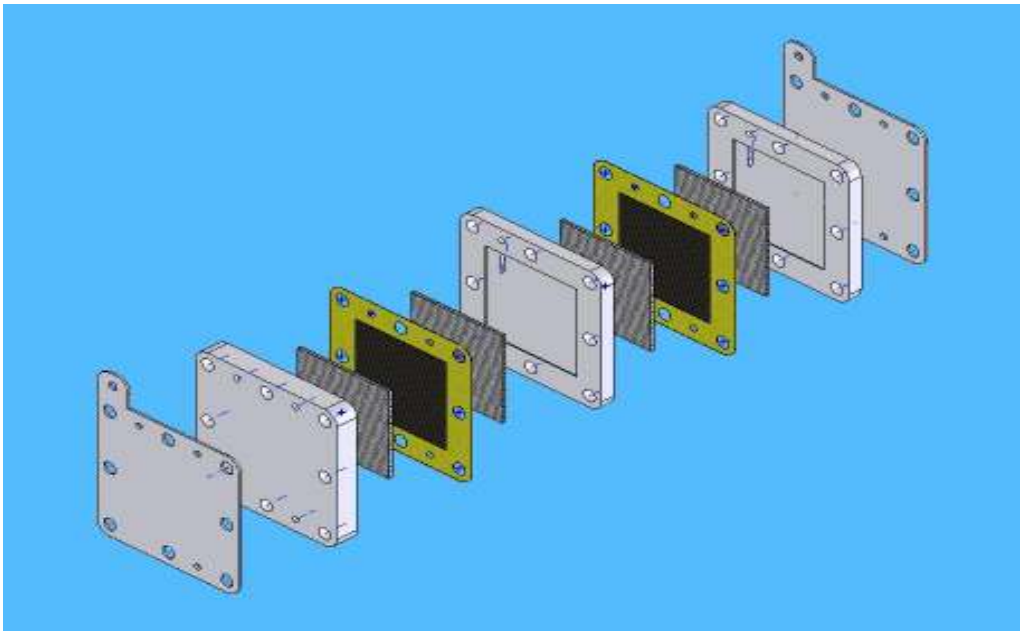

Figure 3.8. Two cell electrolysis stack

Assembly procedure for the multiple cell stack is similar to single cell electrolyzer. The only difference is to repeat some steps of the single cell procedure for each cell. The concept can be used for any cell numbers but many cells in series bring more pressure drop and additional hardware such as high pressure pumps might be required. The stack which was used during the experiments was assembled according to the following procedure.

### 3.2.4 Assembly and Test Procedure for a Multi Cell PEM Electrolyzer

1. Insert 6 bolts to the cathode side end plate and fix the plate to the bench.
2. Place a 1mm thick silicon layer on the end plate.
3. Place the copper electric conduction plate on silicon layer.
4. Place the cathode side graphite.

5. Place the cathode side GDL into the cathode graphite layer.
6. Cover the cathode GDL with 1mm thick silicon gasket.
7. Submerge the MEA into water and wait until the expansion of membrane stops
8. Insert the wet MEA on cathode GDL.
9. Place the anode side GDL on the anode side of the bipolar plate.
10. Cover the anode GDL with 1mm thick silicon gasket.
11. Place the bipolar plate with its mounted components on MEA.
12. Place the cathode GDL into the cathode side of the bipolar plate.
13. Go to step 6 (repeat this step equal to the "number of cells -1" in the stack)
14. Place the water inlet, hydrogen and oxygen outlet graphite plate.
15. Place the copper plate on anode graphite.
16. Place a silicon layer on copper plate.
17. Fixate the anode side end plate.
18. Insert the cap screws to the bolts and tighten them diagonally.
19. Stick the thermocouple probe on to graphite.

Multiple cell electrolyzers have smaller heat transfer area per active electrolysis area with respect to single cell ones. Thus, the stack electrolyzers tend to get hotter than single cell ones; especially at a low water flow and a high current density. Hot electrolysis surfaces usually damage the membrane thus it should be avoided. To control the water inlet temperature, water reservoir was placed in a constant temperature water bath.

Non-uniform water distribution, contact pressure differences between cells, clogged passage ways may cause voltage and temperature gradient between cells or even the melting of the membrane. So, the aim was to operate all the cells of the stack at the same current, voltage and temperature. This requires proper water distribution and gas collecting through all the cells of the stack. Applied current and water feed were kept the same as the previous experimental sets but the occurred electrical potential or temperature of the cells due to less heat transfer area were different. Deionized water was fed to the water inlet via peristaltic pump until the water flooded from the oxygen output. The oxygen output was connected to the inlet water reservoir to return the unreacted water. Hydrogen output line

was treated as before. Positive terminal was connected to first plate (from the top), negative terminal was connected to the last plate.

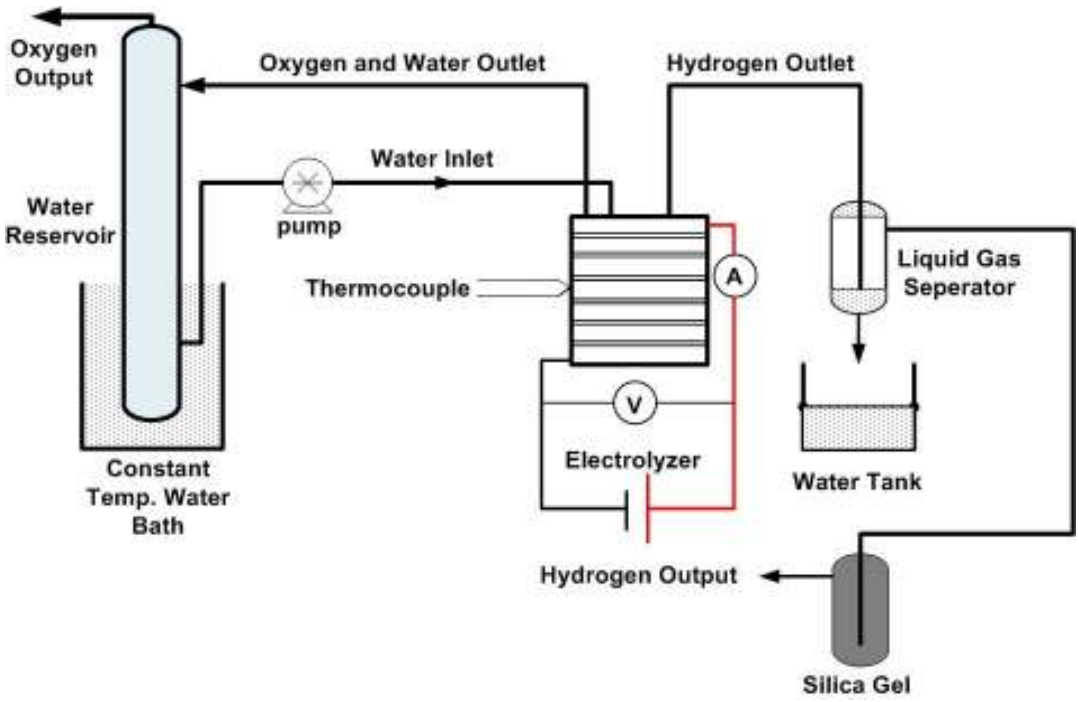


Figure 3.9. Multi Cell Electrolysis Stack Test Setup

### 3.2.5. Assembly and Test Procedure for the Solar Power Driven PEM Electrolysis Stack

To investigate the solar power driven hydrogen production ability of the proposed cell design 5 cell electrolysis stack was constructed and tested in the same as described in section 3.2.3.

DC power supply was disconnected from the system and the negative terminal of the solar array was connected directly to the last plate (cathode end plate) of the stack. Positive terminal of the array was connected to a sensitive $6x10^{-4}$ Ω electric resistance which was then connected to the first plate of the stack in series. A voltmeter was connected to both ends of the resistance to measure the potential difference on the resistance continuously. Dividing the observed potential on resistance gives us the current supplied to the electrolyzer. Another voltmeter was connected to both end of the

electrolyzer to monitor the potential difference of the stack. The solar array consists of six parallel connected Siemens SM-55 photovoltaic modules. The maximum power of one module is 55watt (17.5 Volt and 3.15 Amp) at 20$^{o}$C and 1000W/m$^{2}$ solar radiance according to manufacturer specification sheet. Thus maximum energy output of the solar array is expected as 17.5 Volt and 18.9 Amp for the same operating conditions.

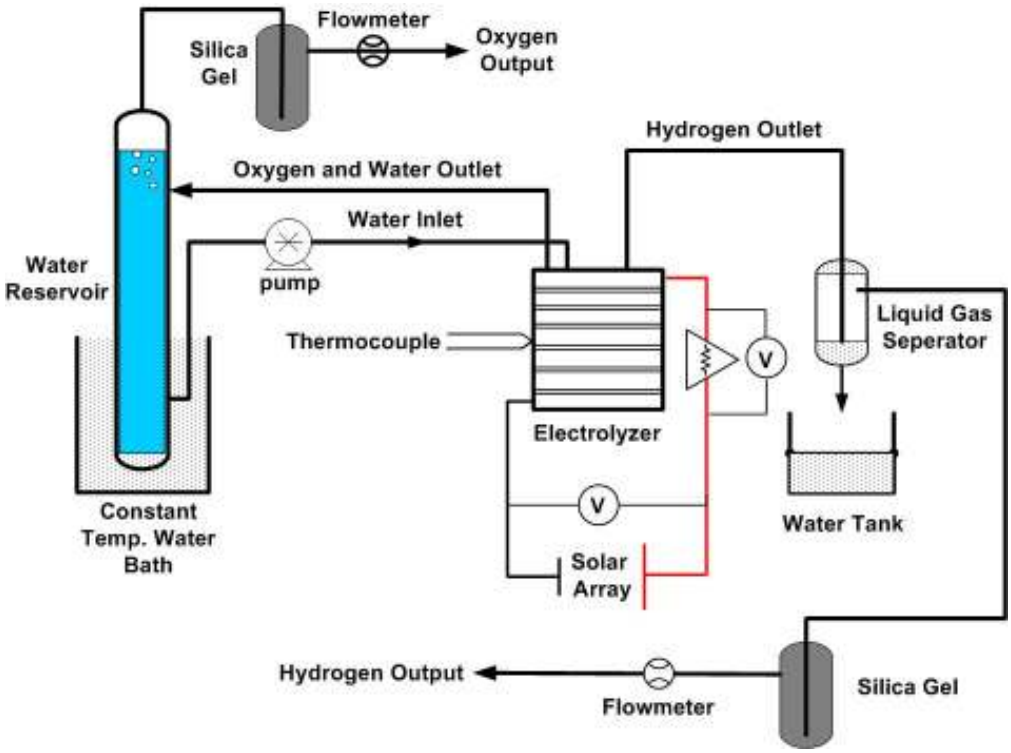


Figure 3.10. Solar power driven electrolyzer stack setup

# CHAPTER IV

# RESULTS AND DISCUSSION

## 4.1 Electrolyzer Manufacturing Experiences on a Single Cell Electrolyzer

Catalyst loadings, cell temperature, operating pressure, various membranes all affect electrolysis efficiency as mentioned in the literature. To construct a properly working electrolysis cell at an acceptable efficiency level, gasket material, flow field design, gas and liquid delivery compartments and the compression level of the cell are also important factors.

The works on the design of inner parts of the electrolyzers in the literature are not given in details and usually did not mention about the compression level of the cell, gasket material, the inside configuration of inlet and outlet gas compartments and the flow field on the graphite layer. In this work, before investigating the performance of the solar power driven proton exchange membrane electrolyzer, research effort was first focused on the construction of a properly working single electrolysis unit.

The design of the cell was improved from experiences gained from the design at hand. During these trials, the shape of the fluid flow field, gasket materials, compression bolts, the formation of gas and liquid chambers were changed step by step.

Seven different electrolysis cell designs were tested. In these trials, water flow rate was set to 2g/min while the temperature of the cell was kept constant at $30^{o}C$. Identical MEA and GDL were used while their active electrolysis areas were $20cm^2$ in all these experiments.

In the first trial, a graphite layer having an “X” shape flow pattern was machined as shown in figure 4.1.

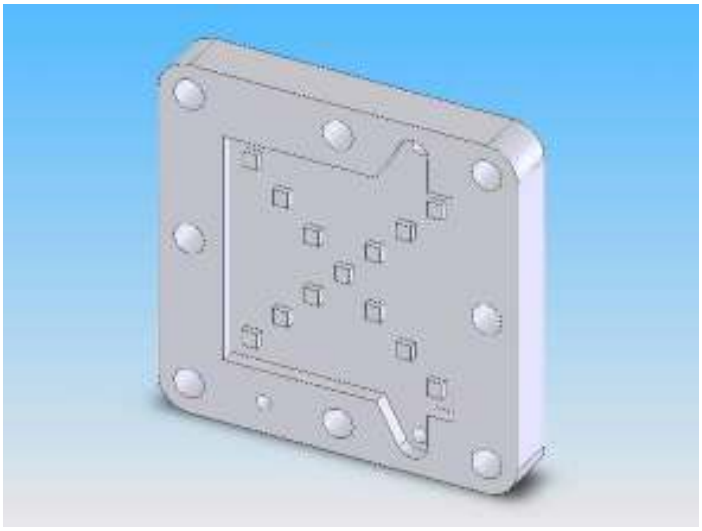

Figure 4.1. “X” type flow field design

The depth of the field was 2mm while the pins were 3mmx3mm squares and 1mm in height. 0.5mm. Rubber gaskets were used as sealing material to equalize the height of the GDL with gasket. Polypropylene bolts having 5mm diameter were used to avoid short circuit between cathode and anode. Water feeding to the electrolyzer and gas removal were accomplished with horizontally drilled 3mm thick ducts. The bolts were tightened as much as possible. After the completion of the assembly, current was applied to the cell and increased gradually. It was observed that the potential difference, such as 5V at 200mAmp/cm$^2$ current density, was too high to be used in practical applications. Due to this low efficiency, heat production in the cell was high which avoided further experimentation at current densities higher than 200 mAmp/cm$^2$.

At the end of the experiment, the cell was disassembled and it was easily seen that the metal GDL was damaged and curled in an “X” shape similar to its support graphite layer due to non-homogeneous conduction of the pressure. Graphite layer design decreased the usable contact area between MEA and GDL and because of that applied current seems to pass from a small area of pins due to better contact between the membrane and gas liquid distributor.

In the second design, to avoid the non homogeneous pressure distribution effect of the X type flow field, pin type flow pattern was used to distribute compression pressure uniformly. Figure 4.2 is the technical drawing of the pin type flow pattern of cathode.

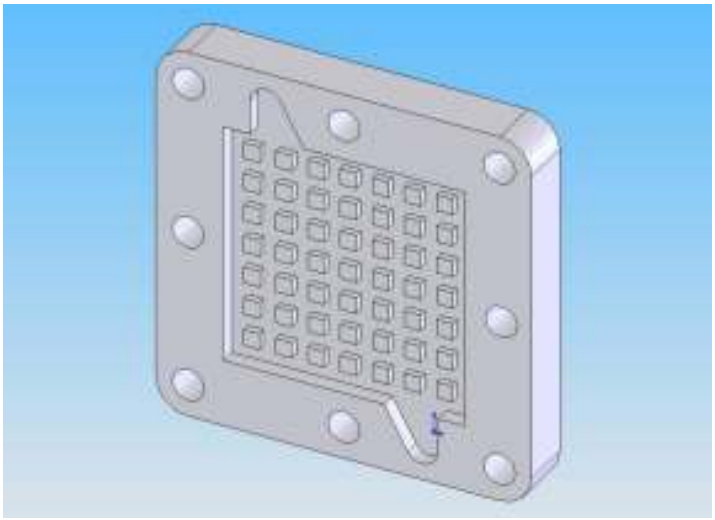

Figure 4.2. Pin Type Flow Field

Except the flow field design, the rest of the materials used in the second design were the same as the first one. The cell was tested under the same conditions and it was observed that the required potential difference decreased to 3.08V at 200mAmp/cm$^2$ which is 38.4% lower than that obtained in the first design. But the voltage efficiency of the cell was still about 48% even at this low current density. During this test, it was noticed that as the bolts getting tighter, voltage of the cell decreased continuously. In fact, 5mm polypropylene bolts could not be tightened more because they could be broken or lose threads.

These tests showed the effect of compression on electrolysis cell that resulted in using thicker bolts with big thread sizes on further trial which tolerated high compression. 6mm polypropylene bolts with big thread were used in the third experiment with all the other materials were the same as the second design. At the same temperature and water flow rate, the potential difference decreased to 2.77V at 200mAmp/cm$^2$ which was 10% lower than that of the second design but still too high for such low current densities according to the results in the literature which were given in chapter two. At the end of the experiment, the cell was dismantled and similar to the X type flow field observations with the first design, the surface of the GDL was not as flat as that in the beginning of the test. On the surface of GDL, the points above the pins were little higher than the areas which were not supported by the pins. Since the deep fields on the GDL cannot contact with

MEA, there were no electrolysis on these areas. Thus, it was decided that further increments on the compression rate would not have a beneficial effect since both GDL's were not able to preserve their flatness at that compression level.

The flow field was changed to an empty flat surface for the fourth electrolyzer cell design. The idea behind the attempt was based on the fact that water and product gases can transport inside the GDL in both horizontal and vertical directions since the GDL was composed of many thin metal screens and there seems to have enough empty space between these metal sheets for the passage of water and gases.

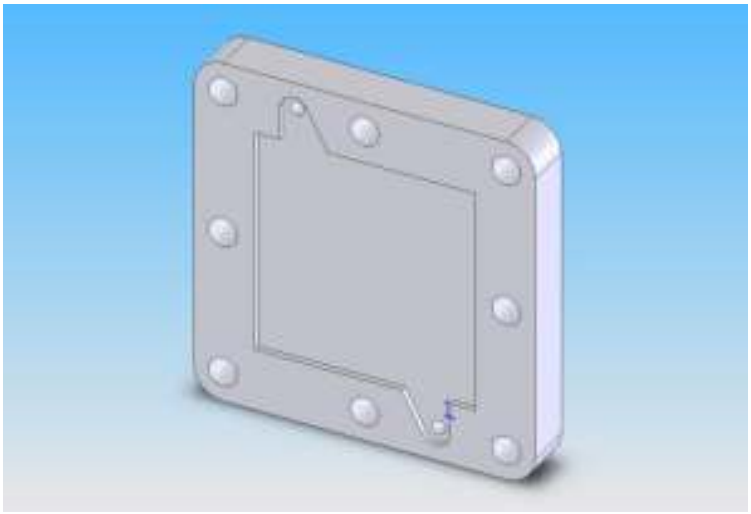

Figure 4.3. Empty Flow Field

Hence, there is no need to put an extra part for the product and reactant transportation behind the GDL. The depth of the empty field was set to 1mm while the rubber gaskets were 0.5mm in thick. The same 6 mm in diameter polypropylene bolts were used for compression. The current was applied to the cell and increased gradually. It was found that this approach seemed to work well. Hydrogen and oxygen GDL's works properly and could remove the product gases as expected. However, there was no voltage usage improvement (2.66V at 200mAmp/$cm^2$) as compared to the previous designs at the same compression levels. After disassembling the cell, it was observed that the flatness of the GDL was preserved. So, it was decided to increase the compression on the cell. Polypropylene is a useful material to be used as a bolt since it is an electrical insulator and

easy to machine. As the higher compression levels were required, the mechanical properties of polypropylene bolts became insufficient. Thus, the steel bolts with plastic covers were used in the further experiments.

In the fifth design, the same graphite layer (shown in Figure 4.3) was used. 5mm diameter metal bolts were used to tighten the cell. Bolts were covered with 6mm plastic tubes having 0.5mm wall thickness to prevent the electrical short circuit between graphite plates. Both graphite plates were covered with a rubber and 5mm thick steel compression plates were placed at the both ends of the cell. Plastic coated metal bolts and rubber gasket covered graphite plates also enabled to protect the experimenter from a hazardous electrical shock during the experiments. Bolts were tightened diagonally and each time every bolt was only turned one quarter in order to prevent the graphite layer from breaking. Similar to previous experiments, current was applied from a power supply to the cell and increased gradually. It was found that efficiency was greatly improved. The required voltage was decreased to 1.93V at 200mAmp/cm$^2$. However, it was observed that the gas flow from hydrogen side was lower than the flow as it should be and also at the same time, the amount of oxygen gas flow was higher than that one would expect. The well tightened cell increases the efficiency up to 77% (according to voltage efficiency) though after dismantling, it was found that the rubber between the plates overflew and intruded from the sides to both of the gas/liquid exit openings inside the active area. The intruded plastic gasket parts tore the membrane and caused the product gases to mix.

In the sixth electrolysis cell design, the gaskets were cut from silicon since silicon sheets were softer than the rubber and it was expected that the silicon would not tear the membrane. Thicknesses of the silicon sheets were 1mm which is the thinnest silicon available in the market. In order to equalize the height of the membrane electrode assembly and gaskets depth of the flow field was machined as 0.5mm. During the experiment, it was observed that the voltage requirement was slightly decreased to 1.88V at 200mAmp/cm$^2$. Better contact surface was obtained between GDL and MEA due to soft gasket material which became thinner than the rubber at high tightening pressure. However, the silicon gasket did not help to solve the gas mixing problem since the gas flows were still not equal to expected hydrogen and oxygen flow rates.

In fact, it was observed on the disassembled cell that there was not any hole or a tear occurred on the membrane, though the gas collection parts located at the top of the graphite was too big and the soft silicon sheet on the top of this part generated an imbalanced pressure on membrane that caused the membrane to stretch from anode to cathode which allowed the gas mixing.

It was decided to remove the gas/liquid exit openings beside the empty field to support the gasket all along the surrounding line of the active electrolysis area. To do that, gas removal and water feed line passages were drilled crosswise from behind the GDL. The graphite plate shown in Figure 4.4 was used in the seventh design.

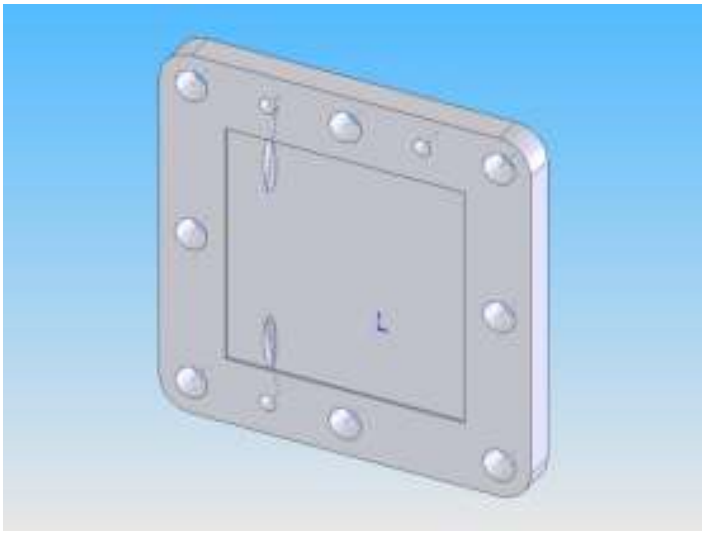

Figure 4.4. Empty Flow field with crosswise ducts

Silicon gaskets were used again while the compression of the cell was provided by plastic covered metal bolts with compression plates as used in the sixth design. In the first step, the cell was tested up to 250mAmp/cm$^2$. The potential difference was found to be 1.80V at 200mAmp/cm$^2$ and also mass balance made on the cell was closed within 3% error. The heat dissipation was very low due to low electrolysis overvoltage. Then, based on the encouraging results, the cell was tested with current densities up to 500mAmp/cm$^2$. The voltage-current characteristic was almost a linear line and the voltage of the cell was measured as 2.20V at 500mAmp/cm$^2$.

The results of all the electrolysis cell designs are given in Figure 4.5.

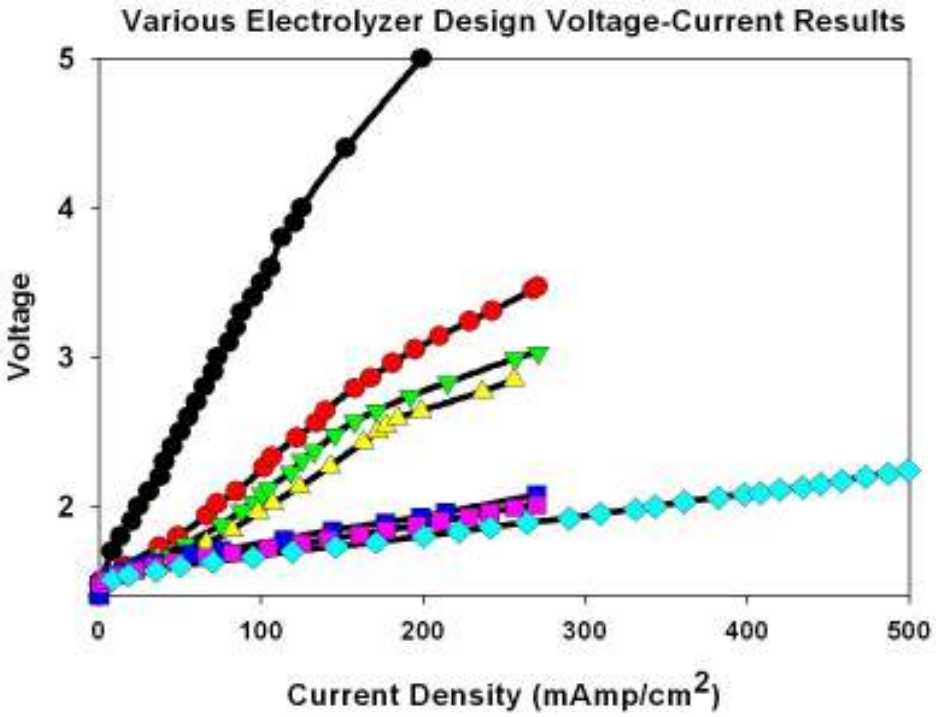


Figure 4.5. Results of Electrolysis Trials

As seen in Figure 4.5, the seventh electrolysis design has a fairly good voltage response and the product gases were not mixed during the experiment. According to that, voltage efficiency of the cell was higher than the previous designs and it was decided to use the seventh design for further evaluation under various water flow rate and operating temperatures.

## 4.2. Results on a Single Cell PEM Electrolyzer

The effects of current density, temperature and water flow rate on the performance of the seventh electrolyzer cell design were examined by 12 sets of runs using the DC power supply.

In each run, current density was increased from 0mAmp/cm$^2$ to 500mAmp/cm$^2$ gradually (0, 10, 25, 40, 55, 75, 100, 125, 150, 200, 250, 300, 350, 400, 450 and 500). In each step, the applied current was fixed and electrolysis was continued for a minute at that current and then, voltage of the cell was recorded.

Temperature and water flow rates were kept constant during each run. Hydrogen and oxygen outputs were calculated continuously according to energy efficiency formulations and also at each run, the gas outputs were measured at 100mAmp/cm$^2$ and at 400mAmp/cm$^2$ to check the mass balance on the cell.

### 4.2.1. Effects of Temperature on PEM Electrolysis

Similar to the previous runs, as the current density increased, high potential differences were required. It was observed that increasing temperature had a favorable effect on electrolysis efficiency since it decreased the potential difference. Voltage of the cell fluctuated between 2.16V and 2.20V with an average value of 2.18V at 500mAmp/cm$^2$ and 30$^o$C. The average voltage decreased to 2.05V and 1.97V under the same current density at 40$^o$C and 50$^o$C, respectively. However, the cell was not successfully tested at high temperatures due to clogging by melted silicon gaskets.

The results were grouped to clearly see the temperature effect, as given in Figure 4.6. (a)-(d). The water flow rates were 1g/min in Figure 4.6(a), 3g/min in Figure 4.6(b), 5g/min in Figure 4.6(c), and 10g/min in Figure 4.6(d).

The inverse correlation between temperature and potential difference seems consistent with the literature. According to the findings of Grigoriev et al., their PEM electrolyzer could generate hydrogen at 500mAmp/cm$^2$ and 30$^o$C with a voltage of 1.80V. The required potential difference decreases to 1.55V at 90$^o$C for the same current density (Grigoriev et al. 2006). The relatively low voltage requirement of their cell as compared to the results obtained in this thesis could be due to the low membrane resistance. They used N-112 membranes which had a thickness of 50μm and almost one third of the membranes used in the electrolyzer of this thesis.

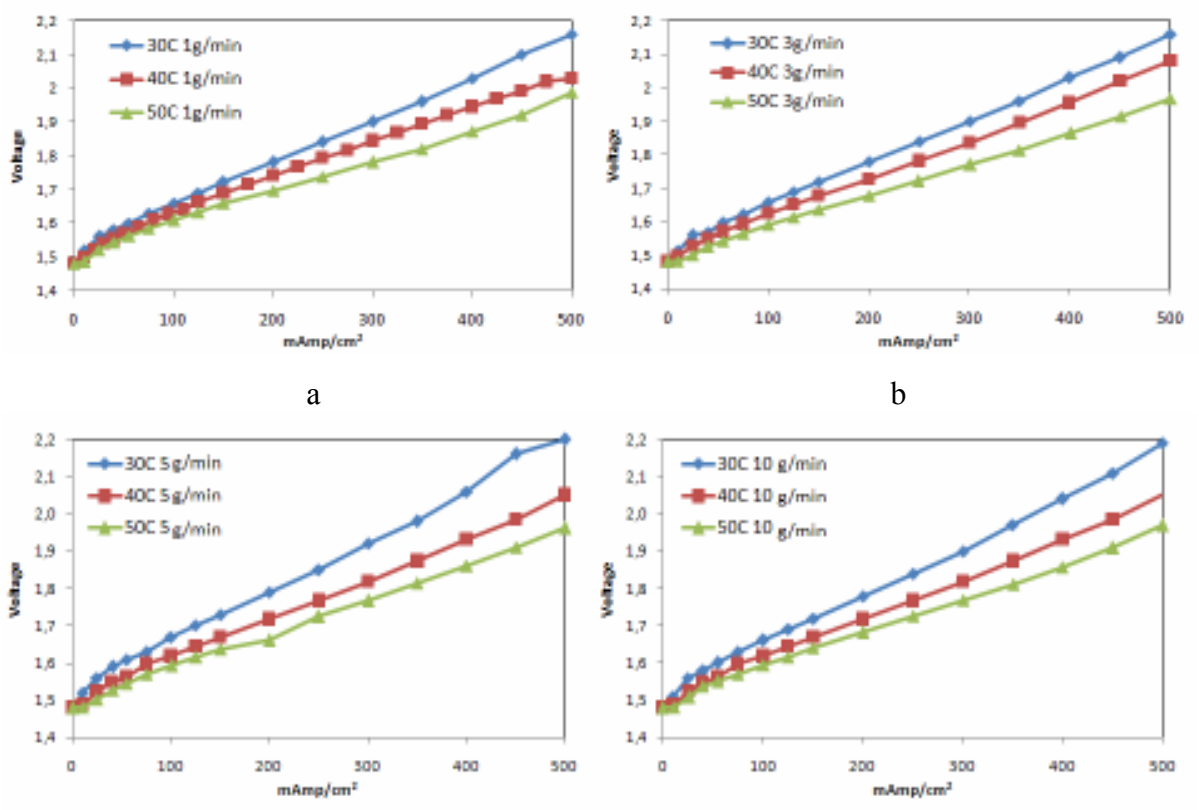


a b

c d

Figure 4.6. (a)-(d) Temperature Effect on Electrolysis

In Figure 4.7, voltage responses of all the cells for varying water flow rates are given at 500mAmp/cm$^2$. The figure shows the relation between temperature and voltage. For all water flow rates, as seen in Figure 4.7, temperature has a positive effect on electrolysis efficiency. In this respect, high cell temperature is advantageous for PEM water electrolysis but with respect to thermal stability of cell components used in this thesis, optimum cell temperature was selected as 50$^o$C. Temperature of the electrolyzers was controlled with an external fan to achieve isothermal operation (as much as possible) at 50$^o$C especially for high current densities.

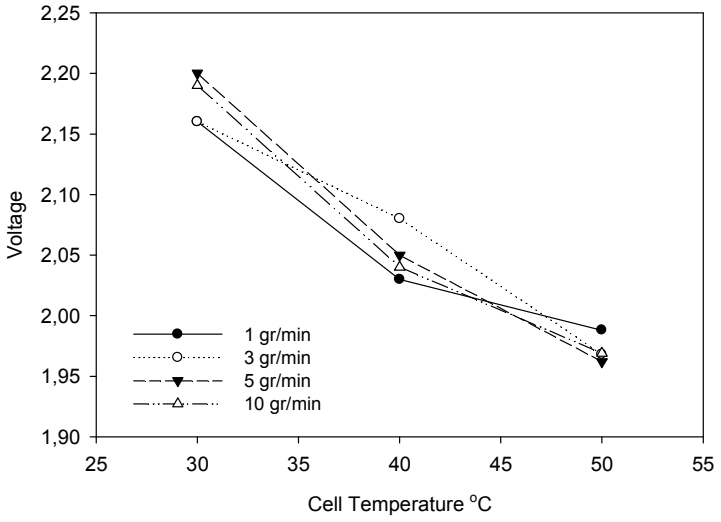


Figure 4.7. Voltage of the cells at 500mAmp/cm$^2$

The temperature increase decreases the cell voltage since both $-\Delta H$ and $-\Delta G$ of the reaction change with temperature. The minimum and the thermoneutral electrolysis voltages also depend on temperature. The situation was indicated by LeRoy and coworkers. They calculated the ideal electrolysis voltage using thermodynamic data. Figure 4.8 plotted using data given in that research study summaries the effect of temperature on both thermoneutral and ideal electrolysis voltage (LeRoy et al. 1980).

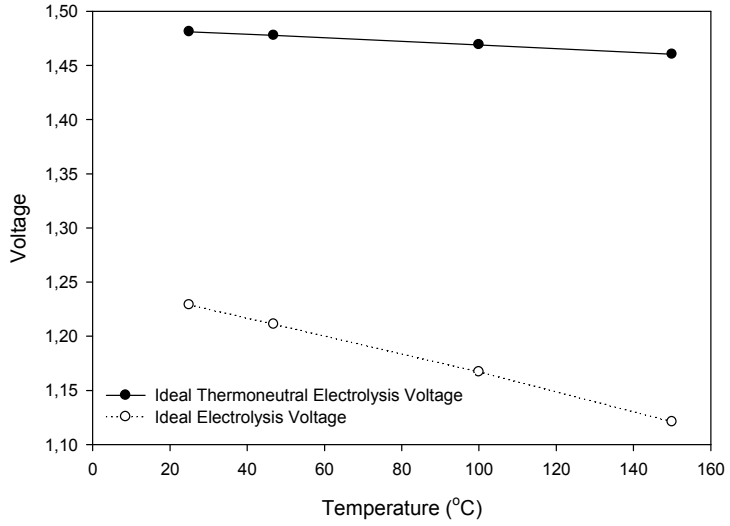


Figure 4.8. Minimum and Thermoneutral Electrolysis Voltage

The thermoneutral electrolysis voltage decreases from 1.481V to 1.477V as temperature increases from 30$^{o}$C to 50$^{o}$C. Similarly, minimum electrolysis voltage decreases to 1.21V from 1.23V for the same temperature interval. However, on an ideal electrolyzer, the change of voltage with temperature is smaller than that found on a non-ideal single cell electrolyzer. High voltage decrements of non-ideal cells with incrasing temperature have other reasons such as decreasing membrane resistance and lower electrode overpotentials due to increasing catalytic activities at elevated temperatures.

### 4.2.2. Effects of Excess Water Flow on PEM Electrolysis

From measured gas output flow rates, it was calculated that actual water converted during the electrolysis was 0,056gr/min at the highest current density. This amount was very low as compared to water fed to the system. So, when the exact amount of water necessary for the electrolysis was introduced into the cell, some problems, such as non-homogeneous electrolysis, occurred. This may be due to that some part of the membrane cannot uniformly be wetted with water.

After the electrolysis started (even the anode side was filled with water at the beginning), the generated oxygen carried away water quickly from the cell when the theoretical minimum water flow rates were used. Especially, it was found that when the cell was disassembled, upper parts of the membrane electrode assembly was dry; indicating that those part was not in contact with water at high current densities if water flow rate was below 1g/min. The situation led to partial melting of the membrane at elevated current levels after a certain time. To overcome this problem, a minimum water flow rate was set as 1g/min and increased to 3g/min, 5g/min and 10g/min to observe the effect of excess water flow rate on the voltage-current density behavior and also the gas flow rates. Since the flow pattern inside the cell has not been studied yet, it is not easy to know how water and gases rates affect each other. In other words, the cell design needs to be optimized by considering flow contact pattern, the catalyst formulation and also types of the materials before stoichiometric water could be used to eliminate the circulation of unused water through the system; hence ultimately decreasing the energy consumed by the circulation water pump.

Therefore, for the current cell design, excess water was used to control the temperature of the cell and also to prevent the membrane electrode assembly from drying.

The experimental results were grouped together to clearly see the effect of excess water flow on the voltage. These are shown in Figure 4.9 (a)-(c). Temperatures were 30$^{o}$C in Figure 4.9(a), 40$^{o}$C in Figure 4.9(b) and 50$^{o}$C in Figure 4.9(c).

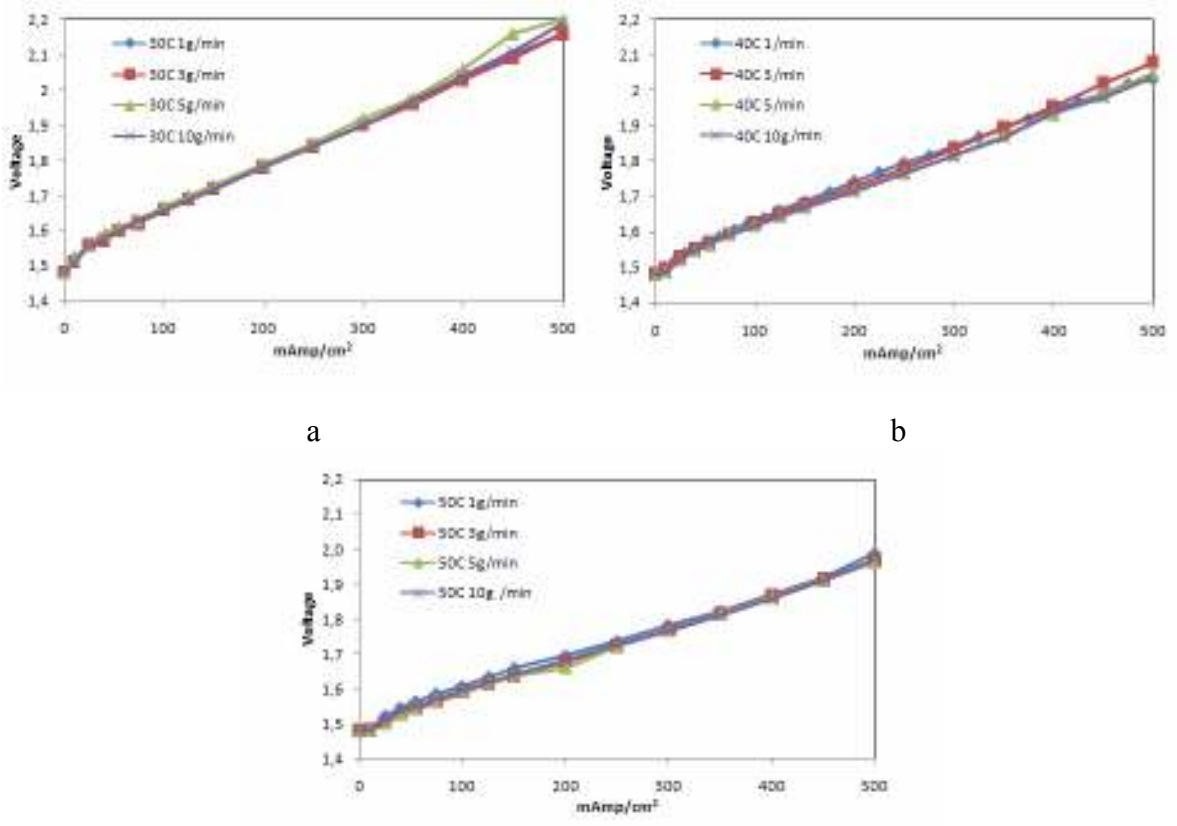


Figure 4.9. (a)-(c) Excess Water Flow Effect on Electrolysis

At 500mAmp/cm$^2$, oxygen flow rate from the cell was 37.5ml/min. At 1g/min water flow rate, 2.5% (by volume) of the output stream coming from anode side was water (the rest was oxygen) and at 10g/min, this fraction increased to 21%. Total liquid volumetric flow rate from the cell increased 23% although oxygen generated was the same at a constant current density. In addition, excess water did not result in adverse effect on the voltage (at a constant current denisty). The main advantage of excess water is to control the temperature of the cell. This is especially critical at high current densities. In other

words, a high water flow rate is necessary to remove the generated heat from the electrolyzer. During the first experiment set (1g/min at 30°C), it was found that the heat removal was low although excess water was used. So, the external fans were used to increase the convection heat transfer around the cell to keep the temperature of the cell constant as much as possible. In all tests, this temperature control strategy (excess water and external fans) was used.

In Figure 4.10, voltage responses of all the experiments at 500mAmp/cm$^2$ are given. The effect of temperature is clearly seen but it can't be concluded that excess water flow has some effect on electrolysis voltage. The voltage fluctuation at the same temperature and varying flow rates were within 0.9% according to the average value at that temperature. The voltage fluctuation with varying flow rates can be presumed within the experimental error region and due to that it can be said that there is no certain effect of increasing water flow rate to the voltage response.

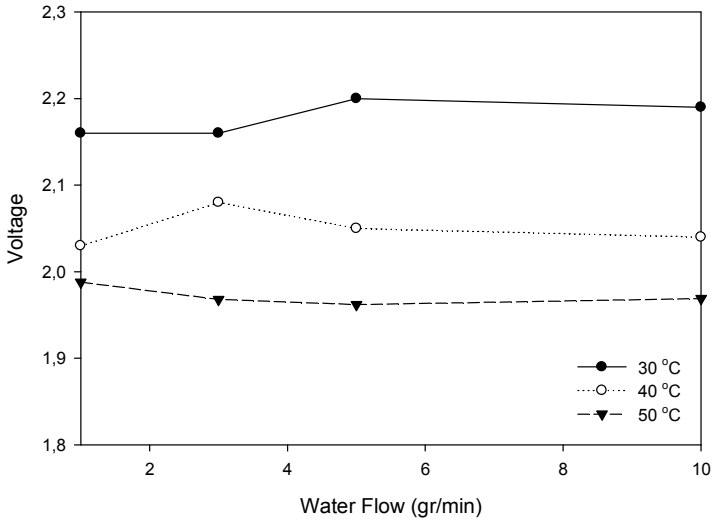


Figure 4.10. Voltage of the cells at 500mAmp/cm$^2$

During the single cell experiments, as mentioned before, hydrogen and oxygen flow rates were measured at 2Amp (100mAmp/cm$^2$) and 8Amp (400mAmp/cm$^2$). Both gas flows were at room temperature (295K) since the gases passed through several apparatus at room temperature. It was calculated that the hydrogen output must be 15.03ml/min and 60.12ml/min and oxygen output must be 7.51ml/min and 30.06 ml/min at 2Amp and

8Amp, respectively. The calculated and measured results are given in Figure 4.11(a) for oxygen flow and Figure 4.11(b) for hydrogen flow.

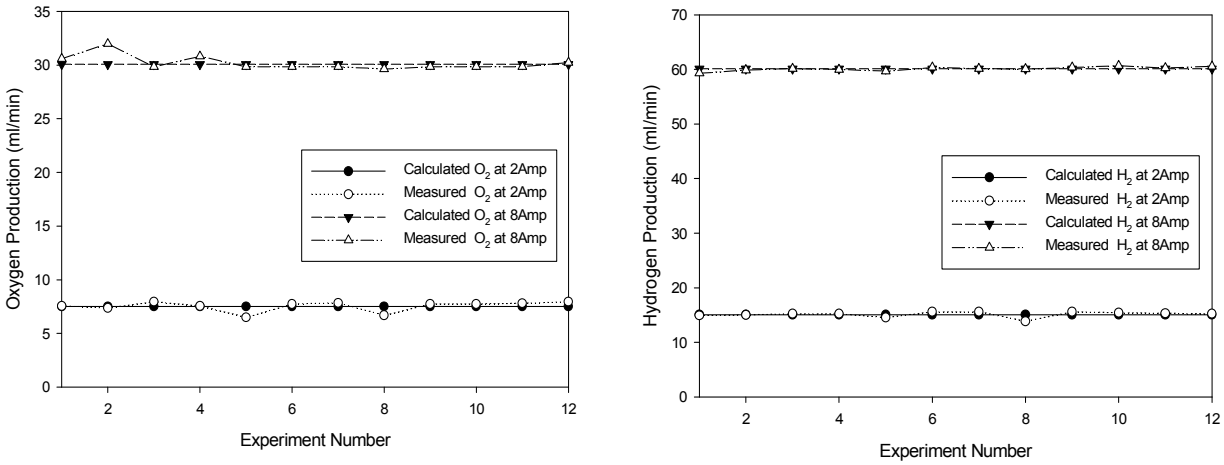


a b

Figure 4.11. Calculated and Measured Oxygen and Hydrogen Flows

Averages of the measured gas output were within 1% range of the calculated values although oxygen output readings fluctuated within 10% range of flow. This might be due to that the excess water and oxygen competed each other to escape from the cell and also oxygen gas bubbled through the upper part of the water reservoir was coming out; resulting in difficulties in flow measurements with the soap flow meter.

The single cell operated at 500mAmp/cm$^2$ shows that the cell can generate hydrogen at 67.9% to 75.2% efficiency. The reason of the change in the efficiency is due to the temperature and non-optimized design of the current cell, though the results seem to be promising as compared to previously constructed alkaline electrolyzer which operated in previous studies at about 3.5V per cell in our institute (Atagündüz, 1993). However, the major drawback of the current design proposed in this thesis is the operating temperature limitation of the materials used to assemble the cell, such as melting of gasket. This problem prevented the cell from being used at high efficiency levels; i.e. at high temperatures.

Moreover, to increase the cell efficiency, thinner proton exchange membranes can be used instead of using N-117 which is 150μm in thickness because voltage drop on membrane was proportional with its thickness. Though thinner membranes such as N-112 (50μm) have higher hydrogen back diffusion rates. Especially at low current densities,

(which is usually the case for photovoltaic powered electrolysis) hydrogen back diffusion results with an explosive gas output on the oxygen line. To avoid that N-117 was selected as proton exchange membrane for this experimental setup.

## 4.3. Results on a Five cell PEM Electrolyzer Stack

A five cell electrolysis stack was constructed according to the procedure as mentioned in the previous chapter. First, the stack was tested with a regulated DC current supply to examine if there is any problem, such as gas mixing, water distribution or voltage distribution between the cells of the stack.

The water flow was set to 10g/min and also external fans were used depending on the current densities so that it was easy to keep the stack temperature at 40$^{o}$C. The supplied current was increased gradually similar to single cell experiments. The voltage response of individual cell in the stack is given in Figure 4.12.

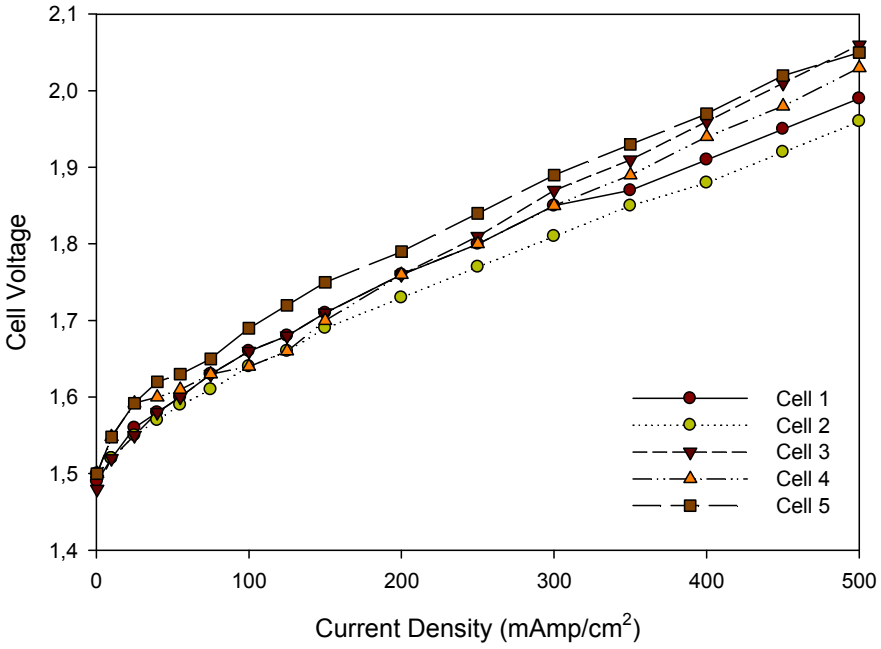


Figure 4.12 Current Voltage Curves of the Cells of an Electrolyzer Stack

At 500mAmp/cm$^2$, the potential difference developed on the stack was 10.09V. The minimum cell voltage obtained across an individual cell was 1.96V (cell 2), the maximum cell voltage was 2.06V (cell 3) and the average cell voltage was 2.018V.

The same assembly procedure was applied to each cell but voltage response of the individual cell was not the same. This might be due to that GDL and MEA in some cells had better contact than the others. Hence, less efficient cells were dissipating more heat than others. This causes a temperature variation between the cells. The maximum temperature was observed as 41.5$^o$C at cell 3 while the minimum was observed at cell 1 as 39$^o$C.

Although the cell voltage response was not identical, the voltage efficiency difference between the most and the least efficient cells was 3.67% at 500mAmp/cm$^2$. The hydrogen output and the voltage of the stack were measured continuously as the current increased. The stack can generate 388ml/min hydrogen at 10Amp (500mAmp/cm$^2$) and 10.09V. Hydrogen generation versus current density and voltage of the stack are given in Figure 4.13.

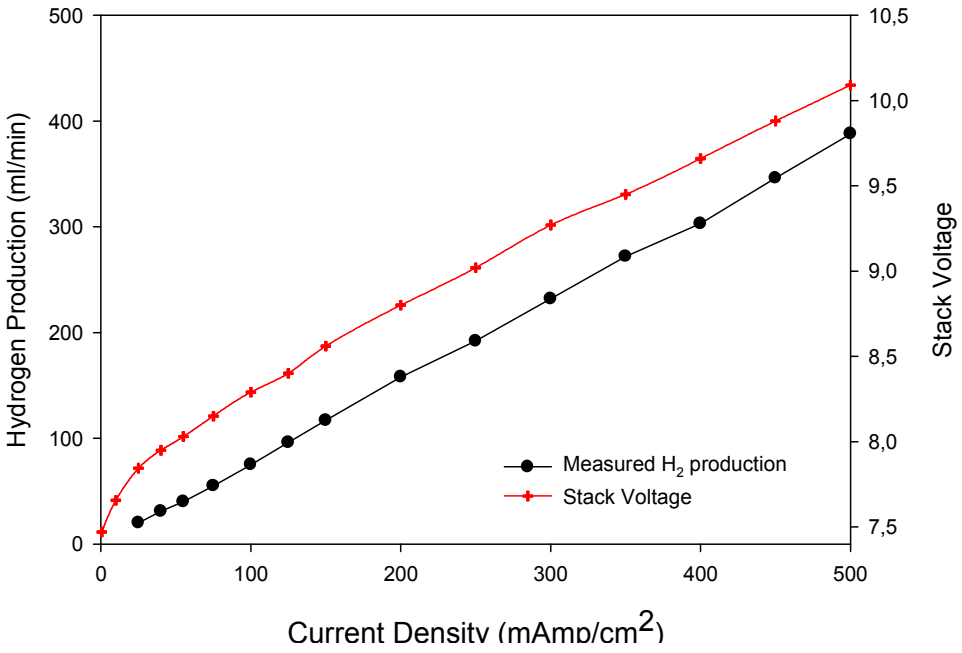


Figure 4.13. Hydrogen Production vs. Current Density

The 5 cell stack was tested for several hours at the maximum possible current density (500mAmp/cm$^2$) supplied by the DC power supply. There were no noticeable fluctuations at the stack temperature, voltage and gas outputs during this test. Mass balance of the stack was also done after reaching steady state (1 hour test at 300mAmp/cm$^2$). It was seen that mass balance could be closed within a 3% error. Detailed information about stack mass balance is given in Appendix B. After that, it was decided to test the cell with a photovoltaic array since this way of hydrogen generation using renewable energy source is the ultimate goal of this thesis.

## 4.4. Results on a Solar Power Driven Five Cell PEM Electrolyzer Stack

Voltage-current characteristic of a photovoltaic panel is affected by solar intensity and the surface temperature of the panel. Voltage-current curves of a Siemens SM-55 PV module was taken from the manufacturer's product specification sheet and given in Figure 4.14. As seen in the figure, short circuit current of a single module is 3.5Amp and the maximum power point of the module is 3.15Amp at 17.4V when solar radiance is 1000W/m$^2$.

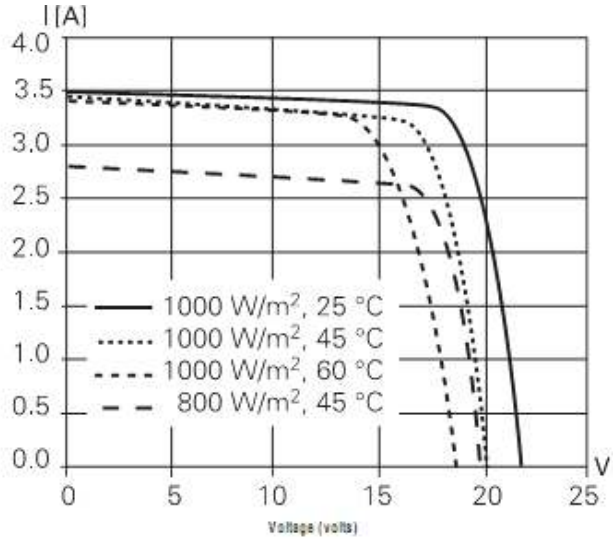


Figure 4.14. Current-Voltage Curves of a PV Module
(Source: Siemens SM55 product specification sheet)

The installed system had 6 of this module connected in parallel. The maximum current of the array was 21Amp and the maximum power point of the array was 18.9Amp at 17.4V when exposed to 1000W/$m^2$ solar radiance at 25$^oC$ panel surface temperature. In fact, at this ambient condition, the array can produce 328W power at its maximum power point. The PV array can supply higher current than the used DC power source GP-1305TP. Therefore, the electrolyzer will be exposed to high current densities up to 1000mAmp/$cm^2$ during the solar powered experiments which means that the heat dissipation will be very high and the temperature control of the stack is very important.

In solar power driven electrolyzer experiments, although water flow was set to 15g/min, the temperature of the stack wasn't constant due to the fast changing weather condition. Moreover, especially heat removal via excess water was not sufficient at high solar radiances due to very high heat dissipation and the stack temperature started to increase rapidly. To prevent the membrane from being damaged at high temperatures, a fan which works at 12V and 0.1 Amp was attached in parallel to the stack. Positive part of the fan's cable was attached to the first anode and negative one was attached to the last cathode. So, the given voltage to the fan was exactly the same with the electrolysis stack. Since the voltage response of the stack changes according to solar radiance, fan revolution was changing accordingly. At high hydrogen production levels, due to high voltage response of the stack, high fan revolutions were observed and increased heat removal was achieved. This configuration prevents high temperature from occurring on the stack at high solar radiances.

The stack was tested for several days from December to June. The solar radiance data and hydrogen production results of some selected days are given in this chapter and the rest of the results are listed in Appendix A.

The stack was tested on 18.12.06 from 8.45AM to 16.15PM. In Figure 4.15, solar radiance data belong to that day is given. The day was partly cloudy as could be understood from the figure. The sharp decrement on solar radiance between 11.00AM and 12.30PM was a result of sun covered by clouds, the low solar radiance decreases the current generation of the array dramatically as represented in Figure 4.14. The highest measured solar radiance was 685W/$m^2$ at 13.30PM.

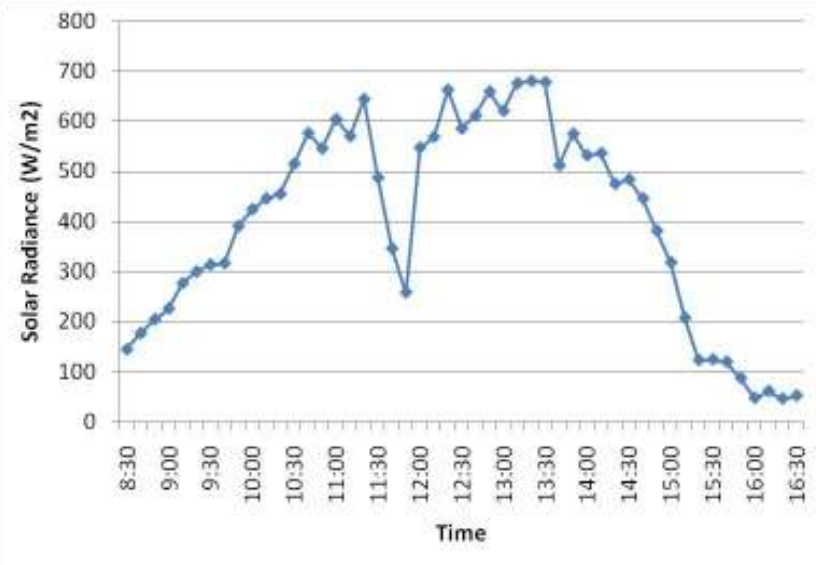


Figure 4.15. Solar Radiance Data on 18.12.2006

As the sun rose, the current increased and reached a maximum value at 12.50PM (13.8Amp) while the stack temperature was 51.7$^{o}$C and voltage was 10.7V. Hydrogen generation was measured as 517ml/min at that time. Figure 4.16 show hydrogen generation and the temperature of the stack during the day.

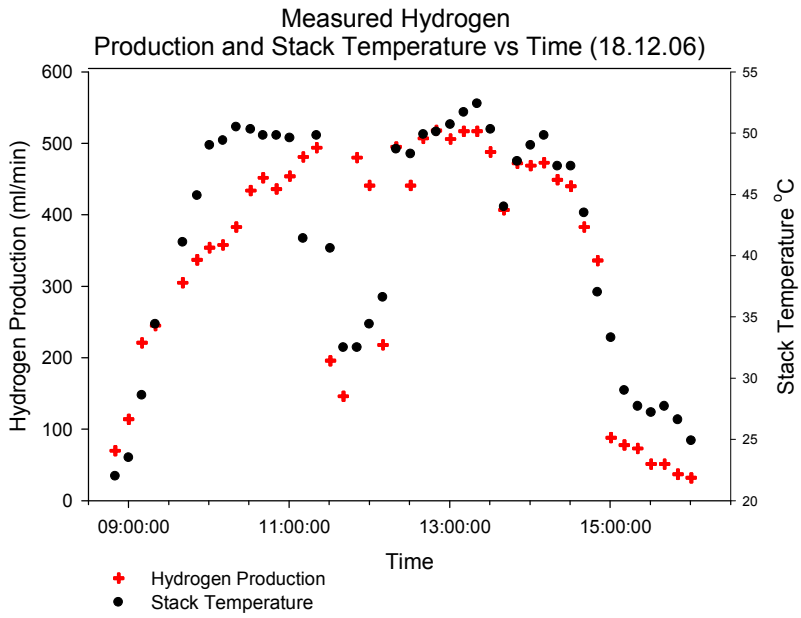


Figure 4.16. Hydrogen Production and Stack Temperature on 18.12.2006

At 11.00 AM, as the current density decreased, voltage requirement of the stack decreased; thus, total power consumption of the stack decreased sharply. The low voltage and current density caused the stack to work at a high efficiency. Most importantly, this lowered the heat generation and the temperature of the stack and the temperature of the stack decreases as a response to that during the cloudy hours.

Another test day was 09.01.07. The electrolysis was performed from 8.45AM to 16.15PM. The day was almost cloudless until 12.50PM. Hydrogen generation and stack temperature decreased after that time and fluctuated as a function of solar radiance. The maximum current was measured as 12.3 Amp at 12.10PM and the maximum hydrogen generation was obtained at this time as 480ml/min. Figure 4.17 shows the hydrogen generation and the stack temperature on that day.

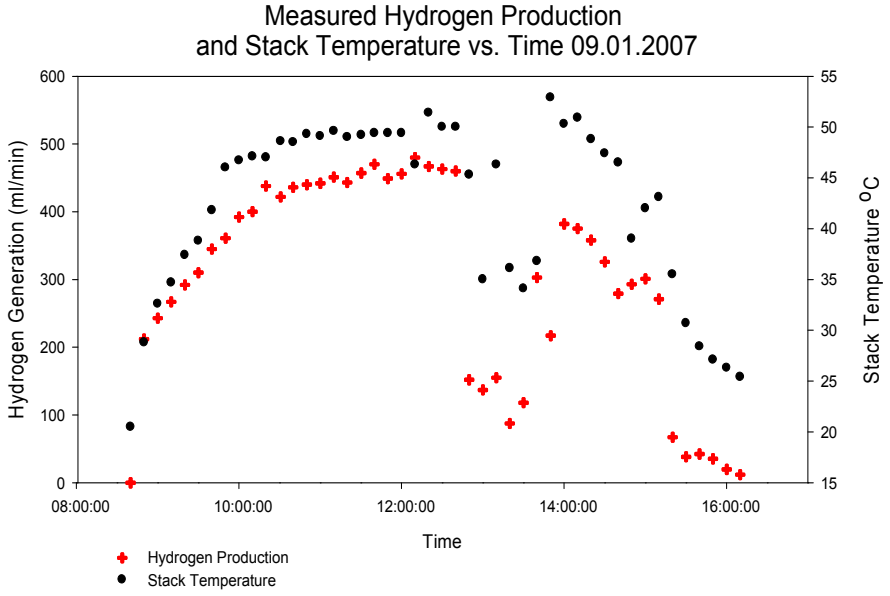


Figure 4.17. Hydrogen Production and Stack Temperature on 09.01.2007

February 22, 2007 was a rainy day and the stack was tested from sunrise to sunset during that day. Solar radiance data of the day is given in Figure 4.18. The highest solar radiance was observed as 780W/m$^2$ at 10.15AM. The rain was started at 10.30AM and continued to 14.15PM, at 15.00PM the rain was started again and continued for the rest of the day.

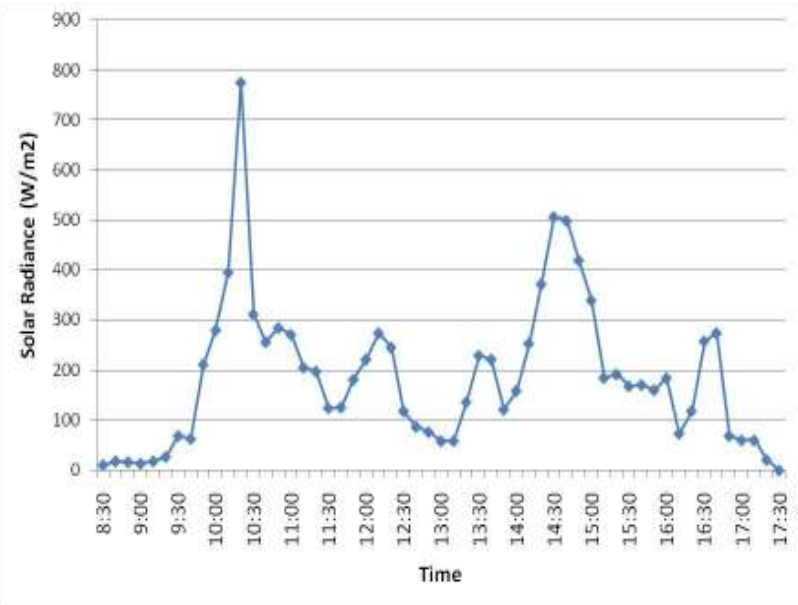


Figure 4.18. Solar Radiance on 22.02.2007

Hydrogen production of the system is given in Figure 4.18. for the same day. On this day, as compared to the previous examples, electrolysis continued up to 17.00PM due to that long day light observed in that month. At the end of the day, total hydrogen production was found to be 55L.

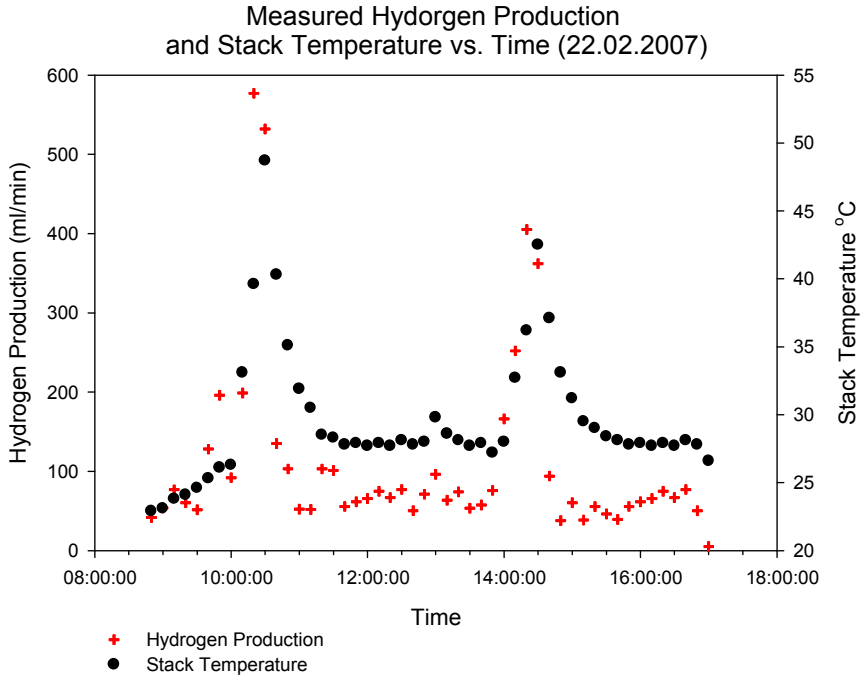


Figure 4.19. Hydrogen Production and Stack Temperature on 22.02.2007

Figure 4.19 shows solar radiance data on Iztech campus on a clear day (14 May 2007). The maximum radiance was observed as 950W/m$^2$ at 13.30PM. Total daylight time which is adequate for electrolysis was about 13 hours.

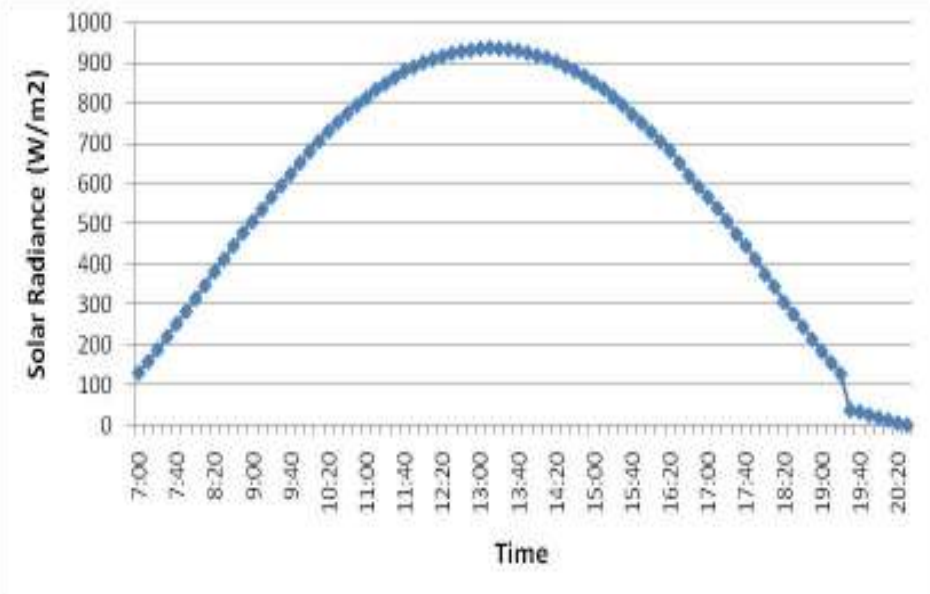


Figure 4.20. Solar Radiance Data on 14.05.2007

The hydrogen production and stack temperature data for the same day is given in Figure 4.20. The maximum hydrogen generation at 13.30PM was measured as 708ml/min. The maximum stack temperature was measured as 53.2$^o$C at the same time. The electrolysis continued up to 20.00PM since day time saving started on 25.03.07. Total hydrogen production was calculated to be 344L at the end of the day.

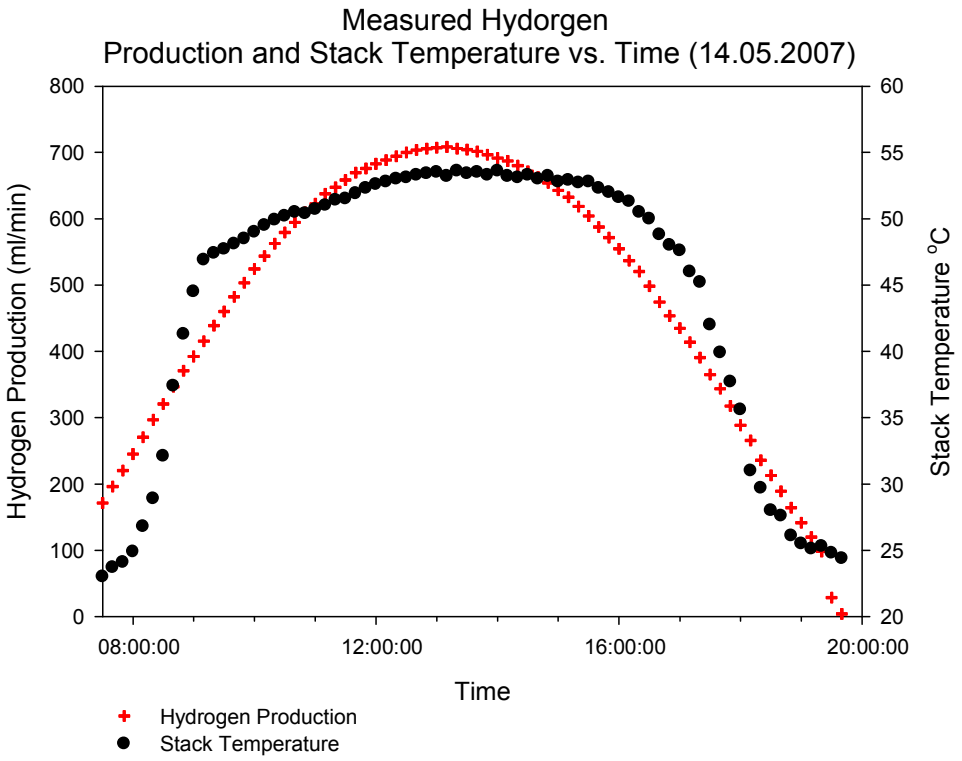


Figure 4.21. Hydrogen Production and Stack Temperature on 14.05.2007

In partly cloudy days, solar radiance fluctuates very rapidly and the temperature of the stack gives a delayed response to that. In some cases, even the hydrogen production was low the stack temperature was almost 50$^{o}$C which resulted in a highly efficient cell operation. But in some cases, the delayed temperature response of the stack became dangerous when the solar radiance increases rapidly the current density increases very fast from a low point to almost 1000mAmp/cm$^2$ within seconds. At that time, the stack exposes to a high current when it is cold. The situation leads a high voltage requirement (less efficient stack) which results in high heat dissipation per unit time. To prevent membrane from melting, even higher water flow rate than that used for previous tests was required. This is the reason why the minimum water flow rate was set to 15g/min flow rate at the solar array powered stack experiments.

As its power source depends on weather conditions, hydrogen production varies from day to day. Minimum daily hydrogen production was observed on 22.02.07 as 55L while the maximum production was 344L at the end of the day on 14.05.07.

On Iztech campus, the system constructed in this thesis can convert up to 4Mj energy equivalent sunlight into chemical energy by producing 28gr hydrogen per day. The efficiency of the stack decreases from 98% to 60% from sunrise to sunset. In addition to that, another energy loss seems to occur between the PV array and the electrolyzer stack. The working voltage of the stack changed between 7.5V to 12.5V which was below that of the PV array maximum power point which is changing between 14.5V to 17.3V according to solar radiance level and panel surface temperature. Due to that, part of the PV voltage capacity cannot be utilized by electrolyzer stack.

# CHAPTER 5

# CONCLUSIONS

The single cell experiments have shown that the flow pattern design and the types of the components used in the construction of the electrolyzers have great influence on the electrolyzer life time and its performance. The cell operating temperature at 500mAmp/$cm^2$ increases the voltage efficiency from 67.9% at 30$^oC$ to 75.2% at 50$^oC$. It was avoided to test the cell at further high temperatures due to gasket melting problem. Various water flow rates have shown that the excess water flow has no influence on the electrolysis cell voltage (i.e. no direct adverse effect on the efficiency) although high water flow rates has made easy to control the cell temperature which is very important especially at high current densities to protect temperature sensitive components of the electrolyzers.

5 cell electrolysis stack was constructed and tested with the regulated power supply. For a constant current density and the stack voltage, the temperature of each cell, hydrogen and oxygen flow rates remain constant and the stack was working properly without any problem. Mass balance made on the cell is closed within 3% error. Though multi cell experiments show that even the components and assembly procedure of all cells are identical, voltage differences up to 5% occur from cell to cell. The situation results in a 2.5$^oC$ temperature difference between the most and least efficient cell in the stack.

The long term usage of the solar array powered 5 cells electrolyzer shows that the applied current to the electrolyzer changes from 0Amp to 20Amp as a function of solar radiance during the day. As a result of that, electrolyzer current density can reach 1000mAmp/$cm^2$ at high solar radiance levels. The voltage drop from 7.5V to 12.5V occurs on the stack based on the current passed through the stack. A maximum hydrogen generation of 750 ml/min could be obtained and also a daily production changes between 50L to 350L according to weather condition of the day.

One of the most apparent way to increase the electrolysis efficiency of the system is to increase the cell working temperature. To provide that, the most heat sensitive material of the system, silicon gaskets must be replaced with heat resistant ones. According to

voltage temperature trend observed in this study and other results in the literature, voltage response of cells will appreciably decrease when the temperature is close to 90$^{o}$C. Though; it should be remembered that as the system temperature increases, hydrogen back diffusion rate will increase.

A torque wrench could also be used to tighten the electrolyzer cells in order to be sure that a uniform compression would be applied to the system. The uniform compression provides the same contact resistance between the membrane electrode assembly and the gas diffusion layer and this will probably cause a decrease in the cell potential. Moreover, with the knowledge of the compression level, the forces applied on each component at high compression rates can be utilized in such way that graphite plates and gaskets can precisely be machined to increase the cell efficiency.

It was observed that the voltage drop on the electrolyzer is much lower than the voltage generation capability of the solar panels. At its maximum power point of the array, voltage can change from 14.5V to 17.3V according to solar radiance and panel surface temperature. This seems to indicate that there is a mismatch between the electric generator and consumer in the system. As a result of that, maximum available energy cannot be transmitted from the solar array to the electrolyzer. To utilize the available voltage potential of the photovoltaic panels, more cell numbered stacks should be assembled and coupled with the array. In addition, since the solar radiance changes as a function of time during the day, the maximum power point of the array changes with time. Hence, this also introduces a mismatch between the array and the "optimized" stack (i.e. stack that works at the maximum power point at the maximum solar radiance possible). To eliminate this type of mismatch, power point tracker could be utilized to maximize the hydrogen production during the day.

As discussed in the previous chapter, especially at rapid change of weather condition, temperature of the cell gives a delayed response to the hydrogen production. The situation results in that the stack exposes to a high current when it is cold; hence, this causes a high voltage requirement of the stack. The design of the cells, liquid-gas flow patterns and the materials of the cell components need to be optimized to be able to respond to the fast changing weather conditions. In fact, total heat capacity of the electrolyzer must be decreased to lower the response time. To do that, graphite plates, which are the parts

with the highest heat capacity in the system, can be replaced with stainless metal plates because metal plates can be machined in much thinner sizes according to graphite and molding or pressing methods could be used for fast and large scale productions.

# REFERENCES


Grigoriev S.A.,Porembsky V.I., Fateev V.N., 2006, "Pure hydrogen Production by PEM electrolysis for hydrogen energy" *International Journal of Hydrogen Energy* 31(2006) 171-175

Yamaguchi M, Horiguchi M, Nakanori T. 2000, "Development of large-scale water electrolyser using solid polymer electrolyte in WE-NET" *Proceedings of the 13th World Hydrogen Energy Conference*, vol. 1, June 12–15, 2000, Beijing, China. p. 274–281.

Tsutomu Oi, Yoshinori Sakaki, 2003 "Optimum hydrogen production and current density of the PEM type water electrolyser operated only during the off-peak period of electricity demand" *Journal of Power Sources* 129(2004) 229-337

Shidong Song, Huamin Zhang, Xiaoping Ma, Zhi-Gang Shao, Yining Zhang, Baolian Yi, 2006 "Bifunctional oxygen electrode with corrosion-resistive gas diffusion layer for unitized regenerative fuel cell" *Electrochemistry Communications* 8 (2006) 399–405

Pettersson J., Ramsey B., Harrison D.,2006 "A review of the latest developments in electrodes for unitized regenerative polymer electrolyte fuel cells" *Journal of Power Sources* 157 (2006) 28–34

Frano Barbir, 2005 "PEM electrolysis for production of hydrogen from renewable energy sources" *Solar Energy* 78 (2005) 661–669

Kazuo Onda, Takahiro Kyakuno, Kikuo Hattori, Kohei Ito, 2004 "Prediction of production power for high-pressure hydrogen by high-pressure water electrolysis" *Journal of Power Sources* 132 (2004) 64–70

Tsutomu Oi, Yoshinori Sakaki, 2004 "Optimum hydrogen generation capacity and current density of the PEM-type water electrolyser operated only during the off-peak period of electricity demand" *Journal of Power Sources* 129 (2004) 229–237

Tsutomu Ioroi, Takanori Oku, Kazuaki Yasuda, Naokazu Kumagai, Yoshinori Miyazaki, 2003 "Influence of PTFE coating on gas diffusion backing for unitized regenerative polymer electrolyte fuel cells" *Journal of Power Sources* 124 (2003) 385–389

Lee S. J., Mukerjee S., McBreen J., Rho Y. W., Kho Y. T., Lee T. H., 1998 " Effects of Nafion impregnation on performances of PEMFC electrodes" *Electrochimica Acta,* Vol. 43, No. 24, pp. 3693-3701, 1998

Kim C. S., Chun Y. G., Peck D. H., Shin D. R., 1998 "A Novel Process to Fabricate Membrane Electrode Assemblies for Proton Exchange Membrane Fuel Cells" *International Journal of Hydrogen Energy* Vol23 No:11 pp1045-1048

Sung-Dae Yim, Won-Yong Lee, Young-Gi Yoon, Young-Jun Sohn, Gu-Gon Park, Tae-Hyun Yang, Chang-Soo Kim, 2004 "Optimization of bifunctional electrocatalyst for PEM unitized regenerative fuel cell" *Electrochimica Acta* 50 (2004) 713-718

Tsutomu Ioroi, Kazuaki Yasuda, Zyun Siroma, Naoko Fujiwara, Yoshinori Miyazaki, 2002 "Thin film electrocatalyst layer for unitized regenerative polymer electrolyte fuel cells" *Journal of Power Sources* 112 (2002) 583–587

Xianguo Li, Imran Sabir, 2005 "Review of bipolar plates in PEM fuel cells: Flow-field designs" *International Journal of Hydrogen Energy* 30 (2005) 359 – 371

Rikukawa M., Sanui K.,2000 "Proton-conducting polymer electrolyte membranes based on hydrocarbon polymers " *Prog. Polymer Science* 25 (2000) 1463-1502

Hankyu Lee, Jiyun Kim, Jongho Park, Yungil Joe, Taehee Lee, 2004 "Performance of polypyrrole-impregnated composite electrode for unitized regenerative fuel cell" *Journal of Power Sources* 131 (2004) 188–193

Rodney L. LeRoy ,Christopher T. Bowen, 1980 "Thermodynamics of aqueous water electrolysis" *Journal of. Electrochemical Society*, Volume 127, Issue 9, pp. 1954-1962 (September 1980)

Brian Russel Einsla, 2005 Doctor of Philosophy in Macromolecular Science and Engineering Thesis Virginia Polytechnic Institute "High Temperature Polymers for Proton Exchange Membrane Fuel Cells"

Gürbüz Atagündüz,1992 " Solar Driven Electrolysis Cell Developed for Hydrogen Production" *Aegean University Solar Energy Institute Publications*

Ahmad G.E., El Shenawy E.T., 2006 "Optimized photovoltaic system for hydrogen Production" *Renewable Energy* 31 (2006) 1043–1054

Hubbert M. King, Shell Development Company Exploration and Production Research Division, Publication No:95 Houston Texas (1956)

Torres L.A., Rodriguez F.J, Sebastian P.J., 1998 "Simulation of a Solar Hydrogen-Fuel Cell System: Results for a different locations in Mexico" *International Journal of Hydrogen Energy* Vol. 23 No.11 pp. 1005-1009

Hoogers, G.,2003 " Fuel Cell Technology Handbook" (CRC Press)

Larminie J., Dicks A., 2003 "Fuel Cell Systems Explained" (John Wiley and Sons)

British Petrol World Statistical Reviews 2006 Energy Outlook

DuPont Product Information Sheet Bulletin No: 97-01 (Rev. 1/4/99) “General Information on Nafion Membrane for Electrolysis

Siemens Solar Industries, Solar Module 55 (SM55) Product Information Sheet

The Annual Energy Outlook 2006, Department of Energy-Energy Information Administration

WEB_1 2006 International Energy Agency Website,
http://www.iea.org/

WEB_2.2005 Department of Energy and Natural Sources Ministry Website
http://www.enerji.gov.tr/

WEB_3.2005 Green Hydrogen Coalition Website
http://www.greenhydrogencoalition.org/

WEB_4 2006 10/04/06 Plastics Technology
http://www.plasticstechnology.com/articles/200201cu3.html

WEB_5 2006 8/01/06 Wikipedia
http://en.wikipedia.org/wiki/Solar_cells

WEB_6 2006 U.S Department of Energy, Hydrogen, Fuel Cells Infrastructure Program
www.eere.energy.gov/hydrogenandfuelcells/production/thermal_processes.html

# APPENDIX A

## HYDROGEN PRODUCTION RESULTS FROM VARIOUS DAYS

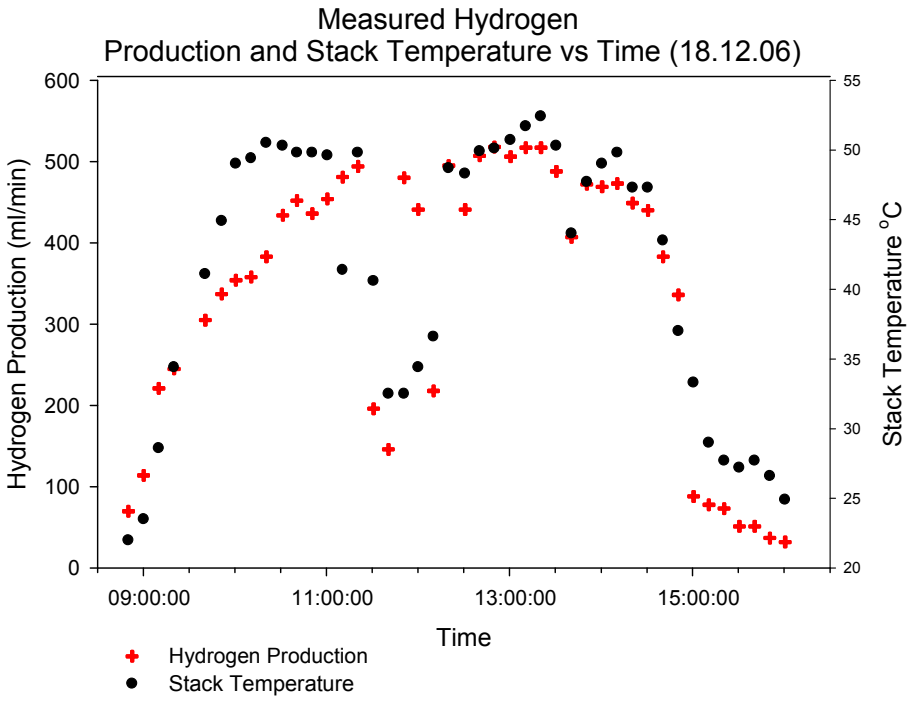


Figure A1

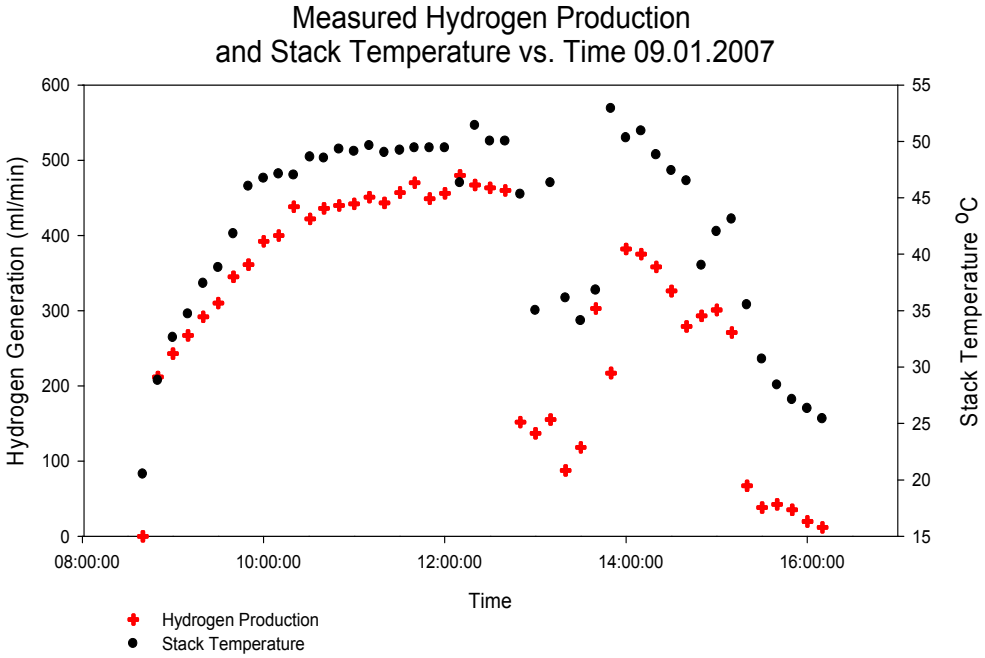


Figure A2

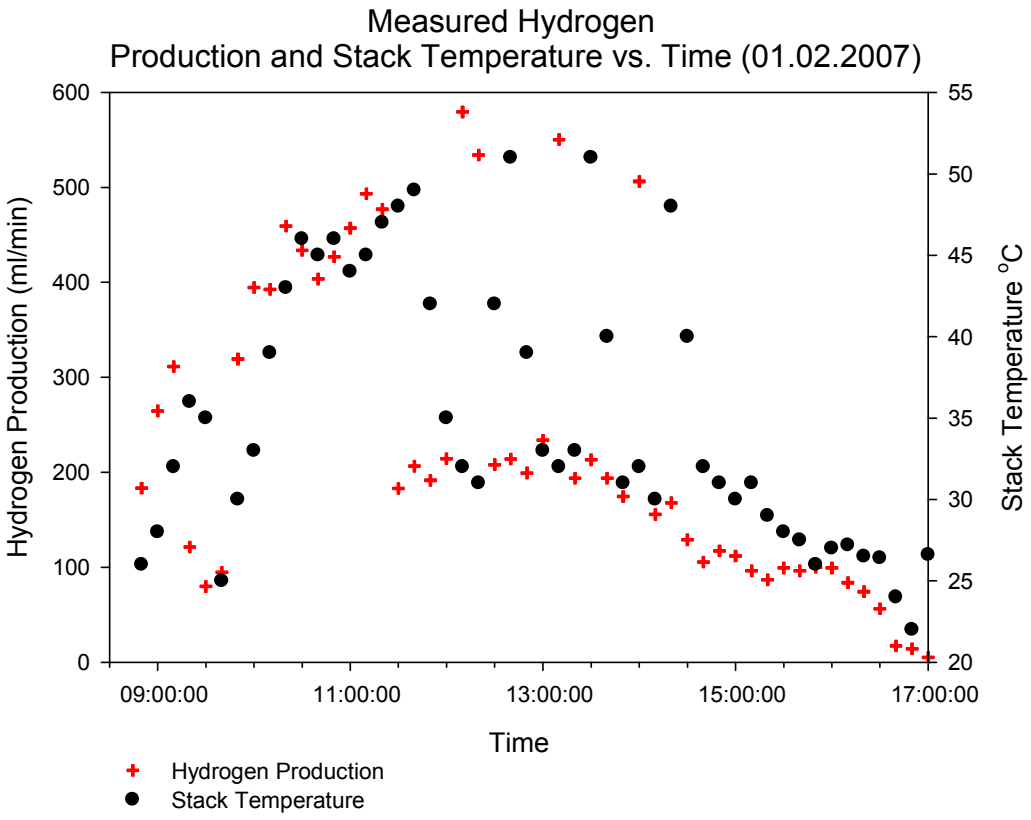


Figure A3

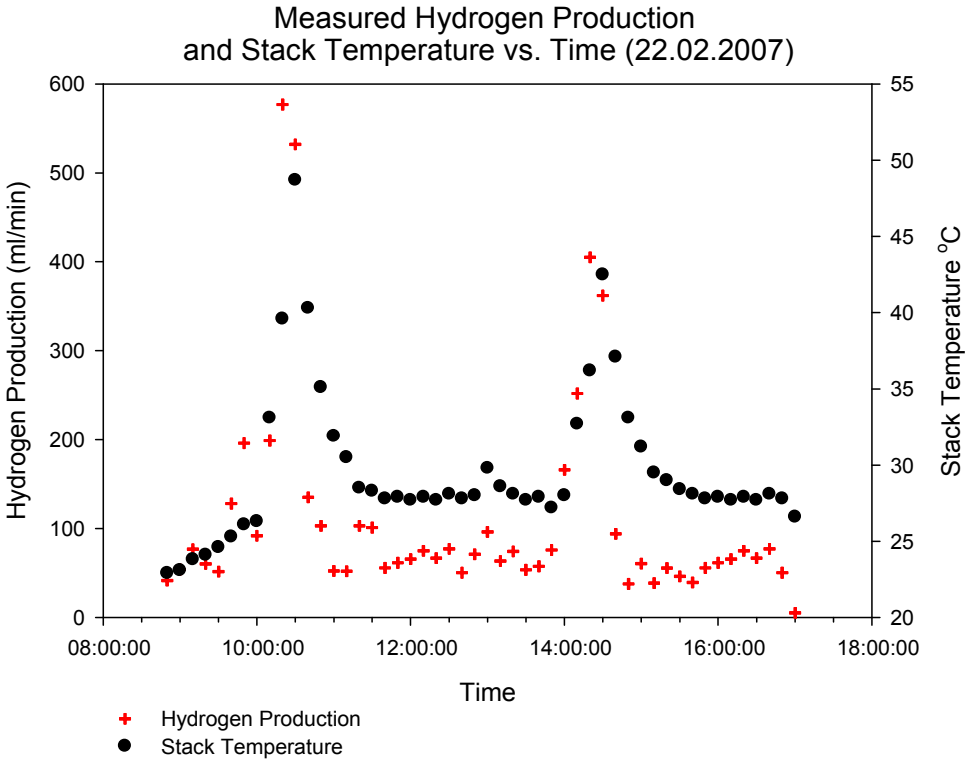


Figure A4

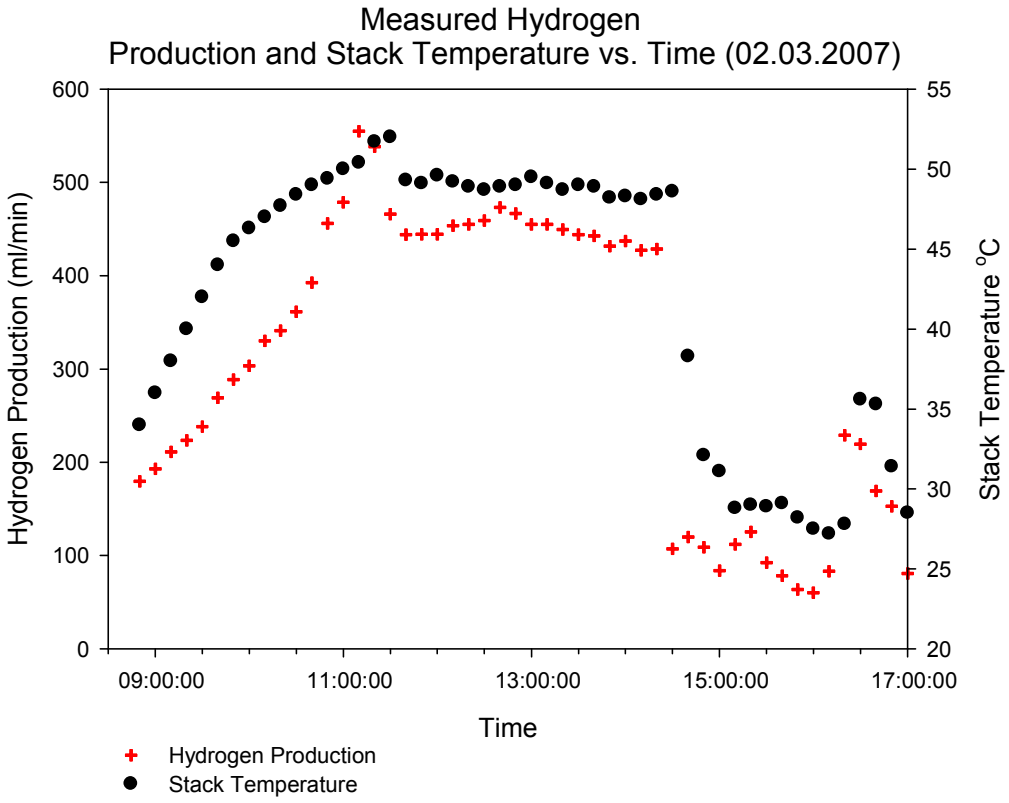


Figure A5

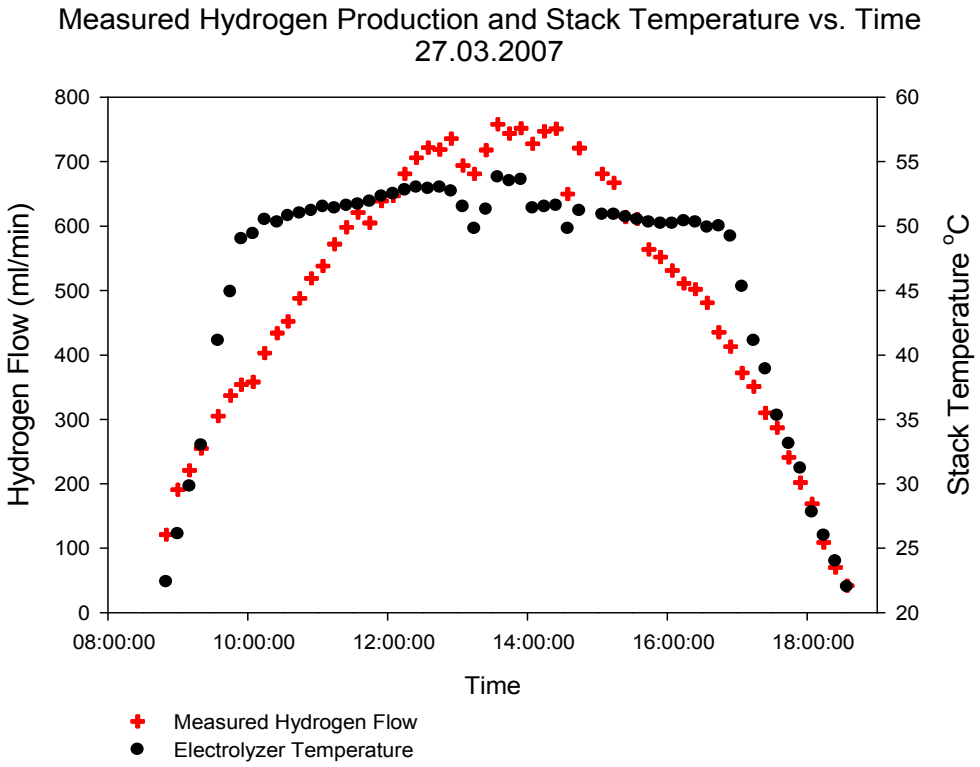


Figure A6

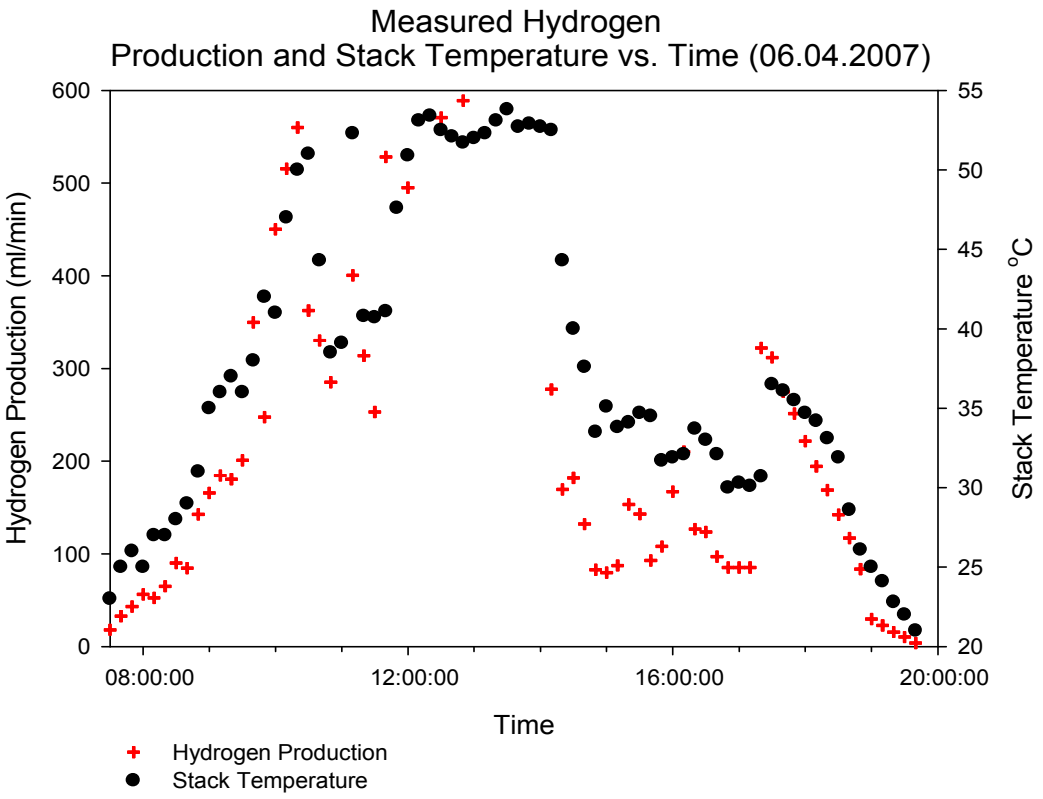


Figure A7

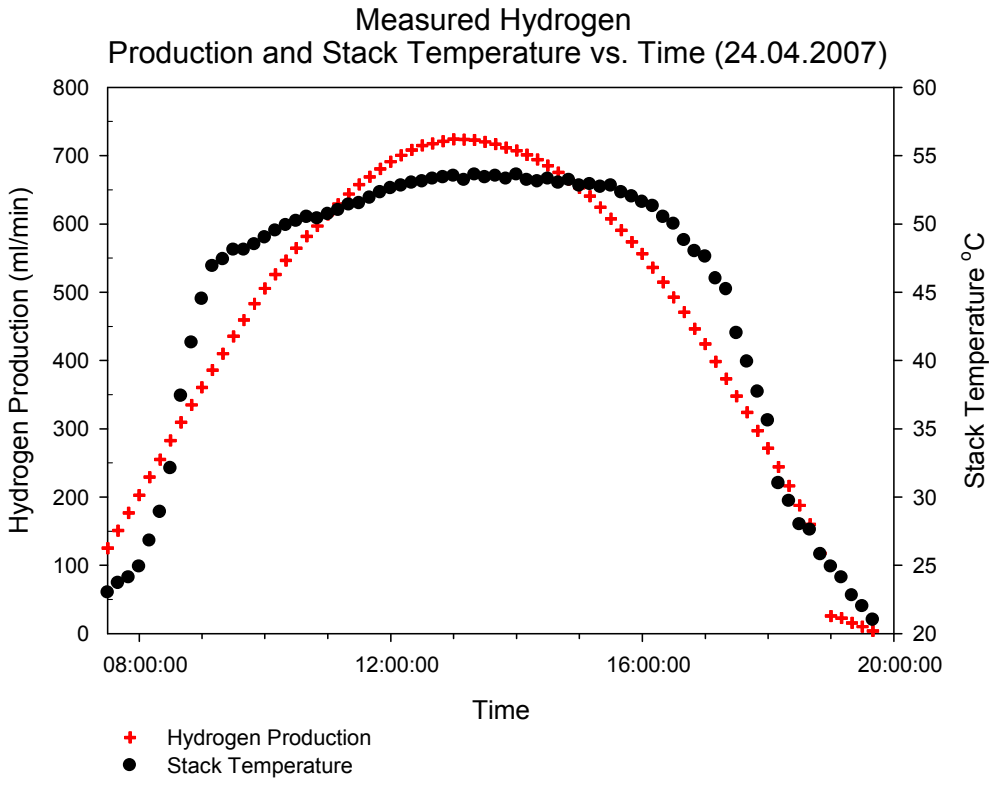


Figure A8

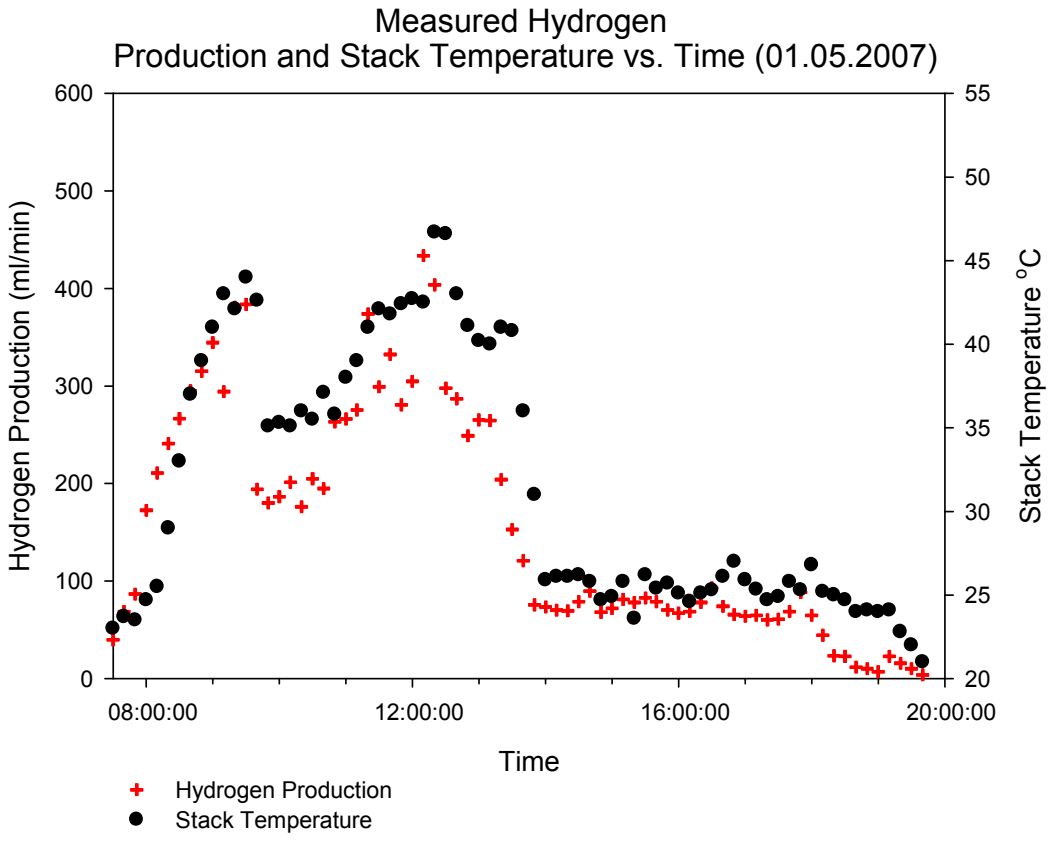


Figure A9

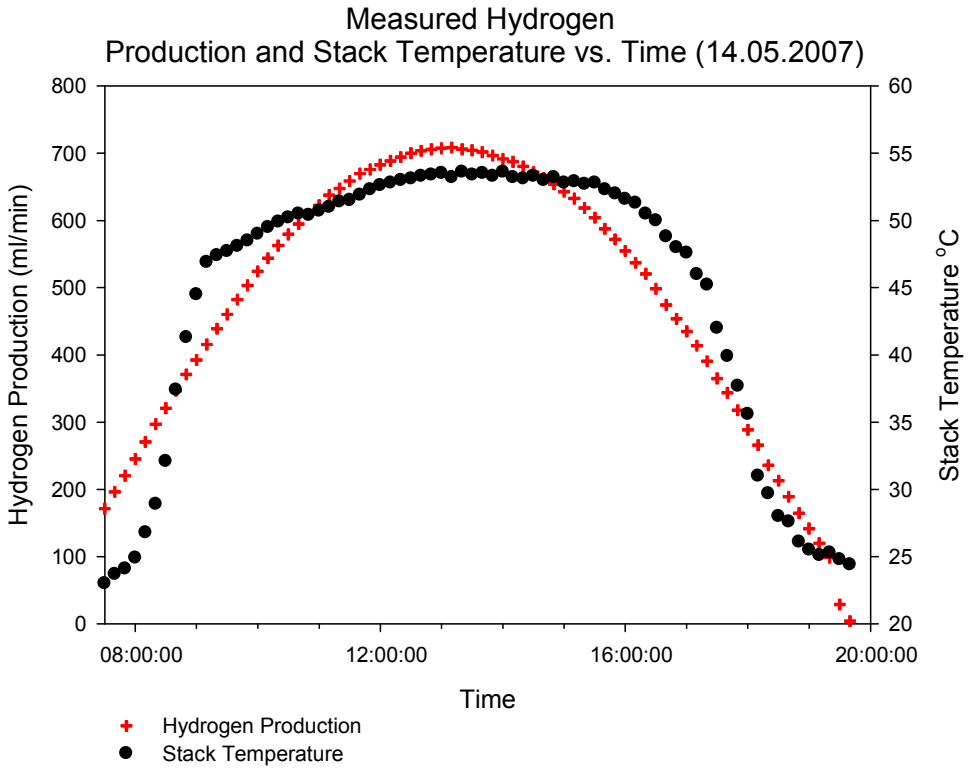


Figure A10

# APPENDIX B

## MASS BALANCE OF A FIVE CELL ELECTROLYZER STACK

The mass balance of a 5 cell electrolysis stack and its auxiliary equipments at steady state is shown here. Flow diagram of the system was given in Figure B1.

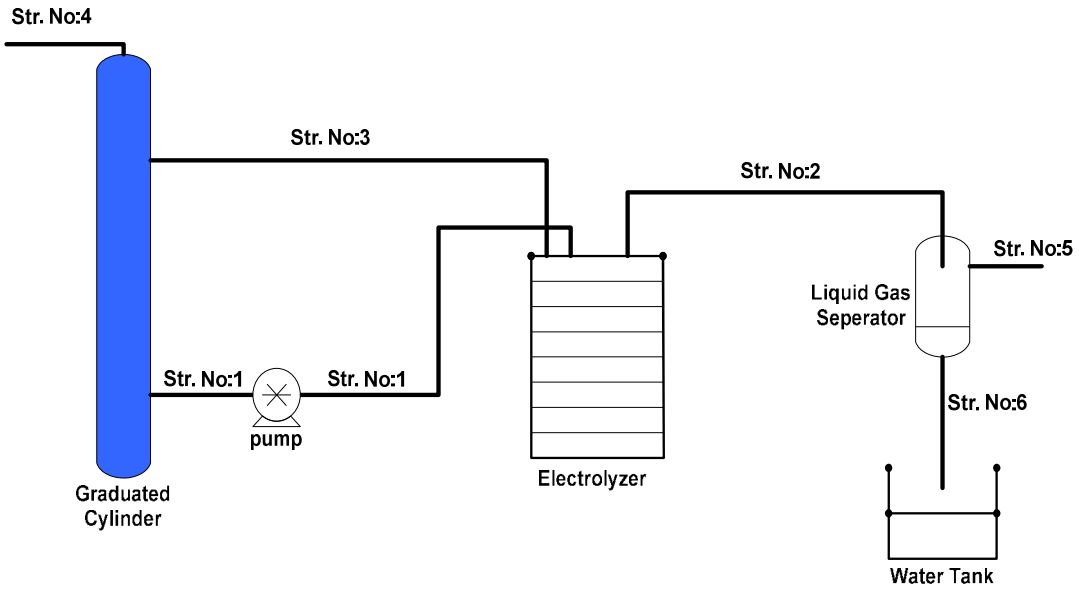


Figure B.1. Stream Numbers of the System

Current, voltage, temperature and streams 1, 4, 5, 6 were the measured parameters. Measured streams and their units were given in the table below.

Table B.1. Measured Stream Units

| Stream No | Stream Name | Unit |
|---|---|---|
| 1 | Electrolyzer water inlet | (gr/min) |
| 4 | Graduated cylinder oxygen output | (15ml/sec) |
| 5 | Gas-Liquid separator hydrogen output | (ml/min) |
| 6 | Gas-Liquid separator water output | (gr/5min) |

Peristaltic pump on stream 1 was set to 10.01gr/min water at the beginning and did not change through the test. Current was set to 6Amp and it was monitored continuously.

Hydrogen output (stream 5) was connected to a digital flow meter while oxygen output (stream 4) was monitored via soap film bubble meter.

In order to provide thermal stability of the setup, system was run for 1 hour before the measurement starts. After that pre-run graduated cylinder was filled with deionized water up to 250ml line. Both electrolyzed water and water permeation through membrane was compensated from the graduated cylinder.

Electrolyzer was operated for 30minutes. Data were taken at the end of 5 minutes interval to see if there was any fluctuation. At the end of the experiment water in the graduated cylinder was 222ml.

Measured Parameters of the experimental setup were given in the table below.

Table B.2. Recorded Outputs of the Steady State System

| Time | Voltage | Current | Temp | Stream 1 | Stream 4 | Stream 5 | Stream 6 |
|---|---|---|---|---|---|---|---|
| | | | C | (gr/min) | ml/min | ml/min | gr/min |
| 11:00 | 9.27 | 6.00 | 41.5 | 10.01 | 113.9 | 226 | ---- |
| 11:05 | 9.27 | 6.00 | 41.4 | 10.01 | 113.9 | 227 | 0.748 |
| 11:10 | 9.27 | 6.00 | 41.5 | 10.01 | 113.9 | 228 | 0.768 |
| 11:15 | 9.28 | 6.00 | 41.6 | 10.01 | 113.9 | 228 | 0.746 |
| 11:20 | 9.27 | 6.00 | 41.4 | 10.01 | 113.9 | 227 | 0.764 |
| 11:25 | 9.26 | 6.00 | 41.5 | 10.01 | 115.3 | 228 | 0.752 |
| 11:30 | 9.27 | 6.00 | 41.5 | 10.01 | 113.9 | 225 | 0.756 |
| **Average** | **9.27** | **6.00** | **41.4** | **10.01** | **114.1** | **227** | **0.756** |

The data show that the system was in steady state during the experiment. Stream 1 and 6 were pure water. Stream 2 and 5 were hydrogen output. Stream 3 and 4 were oxygen outputs. There should be some impurities in these streams such as hydrogen gas in oxygen and vice versa. Also water vapor could exist in stream 2, 3, 4 and 5 with respect to temperature of the flow. Solubility of oxygen and hydrogen gases in water are neglected.

According to these assumptions mass of species in streams were tabulated in the table below. Measured parameters were entered while the unknown parameters represented with capital letters.

Table B.3. Mass Balance of Species on the Overall System

| Mass of Species on Streams | | | | | | | | |
|---|---|---|---|---|---|---|---|---|
| | $H_2O$ | | $H_2$ | | $O_2$ | | | |
| gr/min | Liquid | Gas | Liquid | Gas | Liquid | gas | SUM(gr/min) | measured streams |
| St. 1 | 10.01 | ----- | ------- | ------ | ------- | ----- | 10.01 | 10.01gr/m H2O@298K |
| St. 2 | A | B | ------- | C | ------- | D | A+B+C+D | Unmeasured@314.6K |
| St. 3 | E | F | ------- | G | ------- | H | E+F+G+H | Unmeasured@314.6K |
| St. 4 | ------- | I | ------- | J | ------- | K | I+J+K | 114ml/m gas@298K |
| St. 5 | -------- | L | ------- | M | ------- | N | L+M+N | 227ml/m gas@298K |
| St. 6 | 0.756 | ----- | ------- | ------ | ------- | ----- | 0.756 | 0.756gr/m H2O@298K |

It was measured that water in the graduated cylinder and water output of the gas liquid separator were at 298K. Thus it is assumed that stream 1, 4, 5 and 6 were at the same temperature with their connected equipments. Saturated water vapor pressure is 23.76mmHg at that temperature which resulted 3.13% in stream 4 and 5 as water vapor at 1 ATM. Also, it is reported that N117 membranes can produce both oxygen and hydrogen with 99.5% purity (except water vapor) without any after purification step.

Electrolyzer operating temperature is 314.6K where the saturated water vapor pressure is 58.14mmHg. It was assumed that electrolyzer outputs were also at that temperature. At 1 atm 7.65% of the gas phase of stream 2 and 3 was water vapor. Streams are given in the following tables.

Stream 6 is pure water;

Table B.4. Stream 6

| Species | % | ml/min at 298K | mol/min | gr/min |
|---|---|---|---|---|
| $H_2O$ liquid | 100 | 0.758 | 0.042 | 0.756 |
| Sum | 100 | 0.758 | 0.042 | 0.756 |

It is assumed that all the hydrogen and oxygen gases on stream 2 were separated from liquid water in the liquid gas separator. Thus C=M and D=N

Stream5;

Table B.5. Stream 5

| Species | % of gases | ml/min at 298K | mol/min | gr/min |
|---|---|---|---|---|
| $O_2$ (N) | 0.484 | 1.09 | 4,49E-05 | 1,44E-03 |
| $H_2$ (M) | 96.4 | 218.8 | 8,95E-03 | 1,79E-02 |
| $H_2O$ gas (L) | 3.13 | 7.10 | 2,91E-04 | 5,23E-03 |
| Sum | 100 | 227 | 9,28E-03 | 2,46E-02 |

Since there is no water accumulation in the liquid gas separator mass flow of stream2 is equal to sum of stream 5 and 6.

Stream2;

Table B.6. Stream 2

| Species | %of gases | ml/min at 314.6K | mol/min | gr/min |
|---|---|---|---|---|
| $O_2$ (N) | 0.46175 | 1.15 | 4,49E-05 | 1,44E-03 |
| $H_2$ (M) | 91.88825 | 230.9 | 8,95E-03 | 1,79E-02 |
| $H_2O$ gas (A) | 7.65 | 19.2 | 7,45E-04 | 1,34E-02 |
| Gas Phase Sum | 100 | 251.4 | 9,74E-03 | 3,27E-02 |
| $H_2O$ liquid (B) | --- | 0.74 | 4,15E-02 | 7,48E-01 |
| Total sum | --- | 252.1 | 5,13E-02 | 7,81E-01 |

Stream4;

Table B.7. Stream 4

| Species | % of gases | ml/min at 298K | mol/min | gr/min |
|---|---|---|---|---|
| $O_2$ (K) | 96.386 | 110 | 4,50E-03 | 1,44E-01 |
| $H_2$ (J) | 0.484 | 0.55 | 2,30E-05 | 4,50E-05 |
| $H_2O$ (I) | 3.13 | 3.58 | 1,46E-04 | 2,63E-03 |
| Sum | 100 | 114.13 | 4,67E-03 | 1,47E-01 |

Stream3;

Table B.8. Stream 3

| Species | stream 3 at 314.6K | ml/min at 314.6K | mol/min | gr/min |
|---|---|---|---|---|
| $O_2$ (N) | 91.9 | 116.13 | 4,50E-03 | 1,44E-01 |
| $H_2$ (M) | 0.46 | 0.58 | 2,30E-05 | 4,52E-01 |
| $H_2O$ gas () | 7.65 | 9.66 | 3,75E-04 | 6,74E-03 |
| Sum | 100 | 126.4 | 4,90E-03 | 1,51E-01 |
| $H_2O$ liquid () | --- | --- | --- | E |

Table B.9. Overall Mass Balance on Species

| Mass of Species on Streams | | | | | | | | |
|---|---|---|---|---|---|---|---|---|
| | $H_2O$ | | $H_2$ | | $O_2$ | | | |
| gr/m | Liquid | Gas | Liq. | Gas | Liq. | gas | SUM (gr/min) | measured streams |
| St. 1 | 10.01 | ------ | ------- | ------- | ------- | ------- | 10.01 | 10.01gr/m H2O@298K |
| St. 2 | 0.74 | 1,34E-02 | ------- | 1,79E-02 | ------- | 1,43E-03 | 7,81E-01 | Unmeasured@314K |
| St. 3 | E | 6,74E-03 | ------- | 4,00E-05 | ------- | 1,44E-01 | E+0,1507 | Unmeasured@314K |
| St. 4 | ------- | 2,63E-03 | ------- | 4,00E-05 | ------- | 1,44E-01 | 1,47E-01 | 114ml/m gas@298K |
| St. 5 | -------- | 5,23E-03 | ------- | 1,79E-02 | ------- | 1,43E-03 | 2,46E-02 | 227ml/m gas@298K |
| St. 6 | 0.756 | ------ | ------- | -------- | ------- | ------- | 0.756 | 0.756gr/m H2O@298K |

Remained unknown E represents the liquid water in stream no:3. This quantity can be found from the consumed water from graduated cylinder during the experiment.

$T_{water}$ = 25°C, Density of water at 25°C=0.99707gr/ml

$V_{water}$ at $t_0$ = 250ml, $W_{water}$ at $t_0$=249.2675gr

$V_{water}$ at $t_{30}$ = 222ml, $W_{water}$ at $t_{30}$=221.3495gr

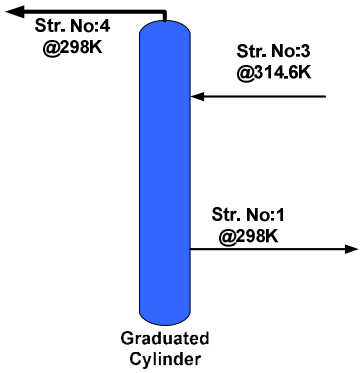


Figure B.2. Input and output streams of the graduated cylinder

Str.No:1 and 4 are the outputs and Str.No:3 is the input.

Table B.10. Calculation of Liquid Water in Stream 4

| | $H_2O$ | | $H_2$ | | $O_2$ | | |
|---|---|---|---|---|---|---|---|
| gr/min | liquid | Gas | liquid | gas | liquid | gas | SUM(gr/min) |
| St. 1 | 1,00E+01 | ------ | ------- | ------- | ------- | ------- | -1,00E+01 |
| St. 3 | E | 6,74E-03 | ------- | 4,50E-05 | ------- | 1,44E-01 | E+0,150753 |
| St. 4 | ------- | -2,63E-03 | ------- | -4,50E-05 | ------- | -1,44E-01 | -1,47E-01 |
| Net | E-10,01 | 4,11E-03 | 0,00E+00 | 0,00E+00 | 0,00E+00 | 0,00E+00 | E-10,0059 |

$$(\mathrm{E} - 10.00589)\, gr/\min \times 30\min = (221.3495 - 249.2675)\mathrm{gr}.$$
$$\mathrm{E} = 9.07529\, gr/\min .$$

Now all the unknowns are known to calculate the mass balance of the electrolysis stack. Inlet stream is No: 1 which is pure water, outlet streams are stream No: 2 and No: 3.

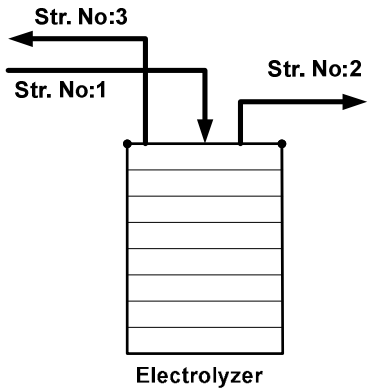


Figure B.3. Input and output streams of the electrolyzer

Table B.11. Validation of the overall mass malance of the system

| Mass Balance on Electrolyzer | | | | | | | |
|---|---|---|---|---|---|---|---|
| | $H_2O$ | | $H_2$ | | $O_2$ | | |
| gr/min | liquid | gas | liquid | gas | liquid | gas | SUM(gr/min) |
| St. 1 | 10.01 | 0 | 0 | 0 | 0 | 0 | 10.01 |
| St. 2 | 7,48E-01 | 1,34E-02 | --- | 1,79E-02 | --- | 1,44E-03 | 7,81E-01 |
| St. 3 | 9,08E+05 | 6,74E-03 | --- | 4,50E-05 | --- | 1,44E-01 | 9,23E+06 |
| NET | 1,87E-01 | -2,02E-02 | 0 | -1,79E-02 | 0 | -1,45E-01 | 3,39E-03 |

According to that total consumed water was 0,167g/min total $H_2$ production was 0.018g/min and total $O_2$ production was 0.145g/min. Conservation of mass was validated within a 2% error for the system.

Net mass flow must be zero to say that there is no accumulation or leakage. Though, it was calculated that there was a little amount of positive net flow on electrolyzer. This might be due to experimental measurement errors such as chronometer timing on oxygen output or reading of volume from the graduated cylinder.

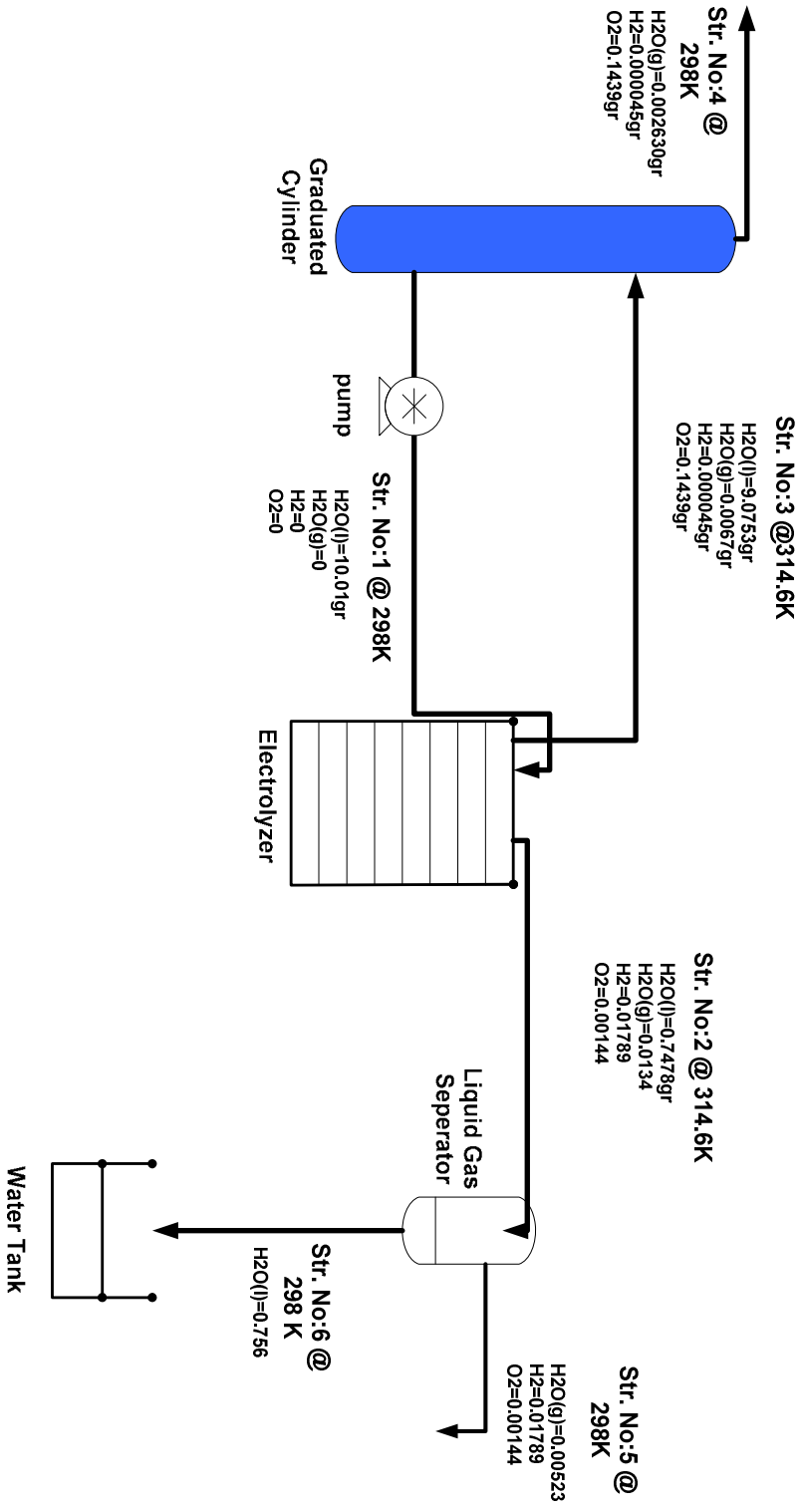


Figure B.4. Overall Mass Balance of the System